Ovarian aromatase loss-of-function mutant medaka undergo ovary degeneration and partial female-to-male sex reversal after puberty

Masatoshi Nakamoto[1,2], Yasushi Shibata[3], Kaoru Ohno[4], Takeshi Usami[4], Yasuhiro Kamei[5], Yoshihito Taniguchi[6], Takeshi Todo[7], Takashi Sakamoto[2], Graham Young[3,8], Penny Swanson[8,9], Kiyoshi Naruse[1*], Yoshitaka Nagahama[10*]

[1.] Laboratory of Bioresources, National Institute for Basic Biology, Okazaki, Aichi 444-8585, Japan.

[2.] Department of Aquatic Marine Biosciences, Tokyo University of Marine Science and Technology, Minato-ku, Tokyo 108-8777, Japan.

[3.] School of Aquatic and Fishery Sciences, University of Washington, Seattle, WA 98195-5020.

[4.] Laboratory of Reproductive Biology, National Institute for Basic Biology, Okazaki, Aichi 444-8585, Japan.

[5.] Spectrography and Bioimaging Facility, National Institute for Basic Biology, Okazaki, Aichi 444-8585, Japan.

[6.] Department of Public Health and Preventive Medicine, Kyorin University, School of Medicine, Tokyo 181-8611, Japan.

[7.] Graduate School of Medicine, Osaka University, Suita, Osaka 565-0871, Japan.

[8.] Center for Reproductive Biology, Washington State University, Pullman, WA 99164-7521.

[9.] Northwest Fisheries Science Center, National Marine Fisheries Service, National

Oceanic and Atmospheric Administration, Seattle, WA 98112-2097.

[10.] Institution for Collaborative Relations, Ehime University, Matsuyama, Ehime 790-8577, Japan.

***Corresponding authors**

Yoshitaka Nagahama

Institution for Collaborative Relations, Ehime University

e-mail: nagahama.yoshitaka.mh@ehime-u.ac.jp

address: Bunkyo-cho 3, Matsuyama, Ehime 790-8577, Japan.

Kiyoshi Naruse

Laboratory of Bioresources, National Institute for Basic Biology

e-mail: naruse@nibb.ac.jp

address: Nishigonaka 38, Myodaiji, Okazaki, Aichi 444-8585, Japan

Abstract

Although estrogens have been generally considered to play a critical role in ovarian differentiation in non-mammalian vertebrates, the specific functions of estrogens during ovarian differentiation remain unclear. We isolated two mutants with premature stops in the ovarian aromatase (*cyp19a1*) gene from an N-ethyl-N-nitrosourea-based gene-driven mutagenesis library of the medaka, *Oryzias latipes*. In XX mutants, gonads first differentiated into normal ovaries containing many ovarian follicles that failed to accumulate yolk. Subsequently, ovarian tissues underwent extensive degeneration, followed by the appearance of testicular tissues on the dorsal side of ovaries. In the newly formed testicular tissue, strong expression of *gsdf* was detected in *sox9a2*-positive somatic cells surrounding germline stem cells suggesting that *gsdf* plays an important role in testicular differentiation during estrogen-depleted female-to-male sex reversal. We conclude that endogenous estrogens synthesized after fertilization are not essential for early ovarian differentiation but are critical for the maintenance of adult ovaries.

62 **Keywords:**

63 Estrogens, aromatase, cyp19a1, ovarian differentiation, sex plasticity, teleost fish

64

65

Highlights

> Two medaka mutants with premature stops in the *cyp19a1* gene were isolated.

>XX mutant ovaries developed normally only through the early developmental stages.

> Ovaries of XX mutants failed to mature and degenerated.

> Estrogen depletion induced partial female-to-male sex reversal in adult ovaries.

> Increased *gsdf* was associated with testicular differentiation during sex reversal.

1. Introduction

Sex steroid hormones (androgens, estrogens and progestins) produced by gonads play critical roles in gonadal differentiation, the maturation of germ cells, and the development of secondary sexual characteristics in most vertebrates. Although many fish exhibit genetic sex determining mechanisms, the genetic program can be overridden by exogenous sex steroids applied during the critical period of differentiation of the indifferent gonad into either testis or ovary, when androgens can induce female-to-male sex reversal and estrogens induce male-to-female sex reversal (Yamamoto, 1969; Nakamura et al., 1998). Therefore, estrogens have been generally considered to play a critical role in the ovarian differentiation of teleost fish. Furthermore, prolonged pharmacological inhibition of estrogen synthesis in adult ovaries by aromatase inhibitors induced functional female-to-male sex reversal in Nile tilapia, medaka and zebrafish (Paul-Prasanth et al., 2013; Takatsu et al., 2013). Therefore, estrogens are key factors in the sexual plasticity of adult ovaries. However, the specific functions of estrogens during ovarian differentiation / development remain unclear.

In steroid-producing cells of gonads, steroid biosynthesis begins with the transport of cholesterol from the outer to the inner mitochondrial membrane by steroidogenic acute regulatory protein (StAR). In both testis and ovary, cholesterol is then sequentially transformed by the following enzymes: cholesterol side-chain cleavage cytochrome P450 (P450scc, CYP11a1), 17α-hydroxylase / 17, 20-lyase cytochrome P450 (P450c17, CYP17), 3ß-hydroxysteroid dehydrogenase / Δ5-Δ4 isomerase (3ß-HSD, HSD3b) and 17ß-hydroxysteroid dehydrogenase (17ß-HSD, HSD17b) to produce various androgens. In the ovary, these androgens are further transformed by cytochrome P450 aromatase (P450arom, CYP19a1) to produce

100 estrogens, predominantly estradiol-17β. Thus, aromatase is a key factor in the
101 biosynthesis of estrogens (Young et al., 2005; Nagahama and Yamashita, 2008;
102 Lubzens et al., 2010).

103 The medaka, *Oryzias latipes*, is a highly suitable model organism for
104 investigation of gonadal sex differentiation in lower vertebrates. The expression of
105 the sex-determining gene *dmy* / *dmrt1bY* is initiated from stage 36 (developmental
106 stage described in Iwamatsu (1994) in genetic male gonads (Matsuda et al., 2002;
107 Nanda et al., 2002; Kobayashi et al., 2004). The first morphological difference
108 between male and female gonads is discernible at Stage 38 (one day before
109 hatching) by the greater numbers of primordial germ cells in female gonads
110 (Hamaguchi, 1982; Satoh and Egami, 1972; Kobayashi et al., 2004). Oogenesis is
111 initiated just after hatching and the ovarian cavity develops at around 20 days after
112 hatching (Kanamori et al., 1985). The initial expression of steroidogenic enzymes
113 was detected in the interstitial cells located on the ventral side of gonads from five
114 to ten days after hatching (Suzuki et al., 2004; Nakamura et al., 2009; Nakamoto et
115 al., 2010, 2012). In medaka, *cyp19a1* is expressed only in the interstitial theca cells
116 and not in ovarian follicle granulosa cells of the developing ovary (Nakamura et al.,
117 2009). These results suggest that endogenous estrogens that are synthesized just
118 after hatching are not essential for early ovarian differentiation in medaka.
119 Conversely, oral or water-borne administration of estrogens during the embryonic
120 period induced functional male-to-female sex reversal in medaka, as in other teleost
121 fish (Yamamoto, 1953; Yamamoto, 1959; Iwamatsu, 1999; Suzuki et al., 2005).
122 However, unlike other teleost fish such as Nile tilapia (Nakamura et al., 2003), oral
123 administration of the aromatase inhibitor Fadrozole to female medaka did not
124 induce female-to-male sex reversal (Suzuki et al., 2004). Fadrozole only inhibited

formation of the ovarian cavity and yolk accumulation in ovarian follicles of medaka (Suzuki et al., 2004). By contrast, the oral administration of the aromatase inhibitor Exemestane in adult female medaka induced spermatogenesis in the ovary (Paul-Prasanth, 2013). Therefore, the functions of estrogens in ovarian differentiation in medaka are currently unclear.

To analyze the molecular mechanisms underlying ovarian differentiation which are mediated by estrogens in medaka, we isolated two mutants with premature stops in ovarian aromatase (*cyp19a1*) from an N-ethyl-N-nitrosourea (ENU)-based gene-driven mutagenesis library, and investigated the phenotypes of mutants during gonadal development. As expected, the activity of aromatase was greatly reduced in mutant gonads. The mutant females developed normal ovaries but yolk accumulation was not observed in the ovarian follicles of the adult ovary. Thereafter, spermatogenesis was observed within adult ovaries of the *cyp19a1* mutants. We provide direct evidence that in medaka, estrogens are not critical for early ovarian differentiation but they are essential for the maintenance of ovarian differentiation.

2. Materials and methods

2.1. *Fish*

Two laboratory strains of medaka, *Oryzias latipes* (Cab and d-rR) were used in this study. The Cab strain was used to establish an N-ethyl-N-nitrosourea (ENU)-based gene-driven mutagenesis library (Taniguchi et al., 2006). The d-rR strain was used for back-cross because the genetic sex of this strain can easily be identified by body color. These medaka strains were provided by the National Bioresource Project (NBRP) medaka, Japan. Fish were maintained in aquaria under an artificial photoperiod of 16h light:8 h dark at 27±2 C°. Embryos were staged using morphological criteria (Iwamatsu, 1994). Genetic sex was identified by PCR according to a previous report (Shinomiya et al., 2004). Hatched larvae were transferred to normal tap water and were fed with *Artemia*. All animal experiments were carried out with the approval from the Institutional Animal Care and Use Committees of the National Institute for Basic Biology and the University of Washington.

2.2. *Screening of cyp19a1 mutants in an ENU-based gene-driven mutagenesis library of medaka.*

The medaka ENU-based gene-driven mutagenesis library consists of frozen sperm and genomic DNA derived from 5,771 F_1 males. *Cyp19a1* mutants were screened by sequencing. Exons 2 and 3 of genomic DNA were amplified by PCR using primer set 5'-CTGGACTGGTATTGGCACAGCCAGCAAC-3' and 5'-CAGCACAGTCTGCCACGTGTCAAAATACTTG-3'. Genomic PCR was performed using Takara Ex-taq (Takara Bio, Shiga, Japan). PCR conditions were 2 min at 95°C, 30 cycles of 10 sec at 96°C, 30 sec at 55°C, and 45 sec at 72°C, then 5 min at 72°C.

168 PCR products were purified using ExoSAP-IT reagent (Affymetrix, Santa Clara,
169 CA) and sequencing was performed in both directions with a 3130xl Genetic
170 Analyzer (Life Technologies, Gaithersburg, MD) using primers
171 5'-AACGGAGAGGAGACCCTGAT-3' and 5'-TCTACAGCTACACACCGTCA-3'. The
172 frozen sperm from the mutagenesis library exhibiting mutation in *cyp19a1* were
173 used to artificially fertilize Cab strain females. To clean out other mutations
174 induced by ENU, F_2 heterozygous fish were crossed with the d-rR strain for at least
175 6th generations.
176
177 2.3. *Genotyping of mutants*
178 Genotyping of the *cyp19a1* mutant strain (K164X), one of two mutant strains,
179 was performed by PCR-Restriction Fragment Length Polymorphism (RFLP): a 187
180 bp DNA fragment was amplified from genomic DNA by PCR using the primer set
181 5'-TCAGCTGCATCGGCATGAACGA-3' and
182 5'-CAGGTTTGGCCCAGTCAAAGCTATGTT-3'. PCR conditions were 2 min at 95°C,
183 30 cycles of 30 sec at 95°C, 30 sec at 55°C, and 30 sec at 72°C, then 5 min at 72°C.
184 The PCR product was digested with restriction enzyme DdeI (Roche Diagnostics,
185 Mannheim, Germany) at 37°C for 1hr and electrophoresed using 8% acrylamide gel
186 or MultiNA (Shimadzu, Kyoto, Japan). In the mutant allele, two bands (99bp, 83bp)
187 were detected in the PCR product digested by DdeI. In the wild type allele, the PCR
188 product was not digested by DdeI. Genotyping of the other *cyp19a1* mutant strain
189 (Q182X) was also performed by sequencing. DNA fragments of the mutated region
190 were amplified by a pair of primers (5'-CATCACGTTCTCAAGAACAGAAAA-3' and
191 5'-CTCTTCCTGGGTGTTCCTGTT-3'). PCR condition were 2 min at 95 C°, 35 cycles
192 of 30 sec at 95 C°, 30 sec at 55 C°, and 40 sec at 72 C° and 5 min at 72 C°. The PCR

193 fragments were then sequenced using the specific internal primer
194 5'-GTTTTGGAAGCAAACAAGGACT-3'.
195
196 2.4. *Steroid assays*
197 Ovaries were dissected from adult fish at 3 months after hatching.
198 Heterozygous siblings had started spawning at this time. Steroid hormones were
199 extracted from the gonad samples with a standard ether extraction method, dried
200 under a stream of N_2, and diluted in 0.5 ml assay buffer. Radioimmunoassay (RIA)
201 for estradiol-17ß was performed as previously described (Sower and Schreck, 1982)
202 using an antibody (cross-reactivities: estrone, 2.6%; estriol, 4.2%; testosterone,
203 0.02%; (Korenman et al., 1974) purchased from Dr. Gordon Niswender (Colorado
204 State University, Fort Collins). For the RIA, 0.2 ml of ovarian extract was analyzed.
205 The minimum detectable limit of the assay (defined as ED80) was 31 pg/ml.
206 Testosterone was analyzed by enzyme immunoassay as previously described
207 (Cuisset et al., 1994) using an antiserum generously provided by Dr. S. Zanuy
208 (CSIC, Instituto de Acuiculturea de Torre la Sal, Castellón, Spain). Testosterone
209 antibody cross-reactivities were: 5α-dihydrotestosterone, 30.1%;
210 11-ketotestosterone, 5.2%; 11β-hydroxytestosterone, 3.9%; androstenedione, 2.9%;
211 progesterone, 0.04%; estradiol-17β, <0.1% (Guzmán et al., 2015). The minimum
212 detectable limit (defined as ED80) of the assay was 60 pg/ml.
213
214 2.5. *RT-PCR for detection of vitellogenin gene mRNA*
215 Total RNA was extracted from the liver using an RNeasy Mini Kit (QIAGEN,
216 Hilden, Germany) and first-strand cDNA was synthesized using Omniscript RT kit
217 (QIAGEN, Hilden, Germany) with oligo-dT primers according to the manufacturer's

instructions. PCR was carried out in a 20 µl reaction mixture containing 1 µl of cDNA using Takara Ex-taq (Takara bio, Shiga, Japan). PCR conditions were 2 min at 95°C, 30 sec at 95°C, 30 sec at 55°C and 30 sec at 72°C for 30 cycles; and 5 min at 72°C. Medaka vitellogenin I cDNA (GenBank accession number: NM_001104677) was detected using a primer set of vtg1-F1 5'-TACGGAGCTGCTCAAACAGA-3' and vtg1-R1 5'-ACAGCAGCAGAGGTTCCAAT-3' that amplified 383 bp. Medaka vitellogenin II cDNA (NM_001104840) was detected using a primer set of vtg2-F2 5'-TGAAAGACGCGACTACGATG-3' and vtg2-R2 5'-AGGCTCTGTGCAAGAGTGGT-3' that amplified 392 bp. ß-actin cDNA was amplified as an internal control. Screening was performed in triplicate for each genotype.

2.6. *Histology*

The gonads and larvae were fixed in Bouin's solution. Tissues were dehydrated and processed using standard procedures and then embedded in paraffin. Sections of 5 µm thickness were cut serially, and stained with hematoxylin-eosin according to standard protocols. Circumferences of ovarian follicles in HE sections were measured using ImageJ 1.49q (Abramoff et al., 2004; Schneider et al., 2012) and the diameters of ovarian follicles were calculated. Ovarian follicles were staged using morphological and size criteria (Iwamatsu et al, 1988). In medaka, pre-vitellogenic ovarian follicles are 20-150 µm in diameter, early vitellogenic stage follicles are 151-400 µm in diameter, late vitellogenic stage follicles are 401-800 µm in diameter, and post-vitellogenic follicles have a diameter greater than 801 µm. The diameter of vitellogenic ovarian follicles was reduced approximately 10% because of dehydration after fixation using Bouin's solution.

243

244 2.7. *In situ hybridization*

245 Sense and antisense digoxigenin-labeled RNA probes were generated using *in*
246 *vitro* transcription with a DIG RNA labeling kit (Roche Diagnostics, Mannheim,
247 Germany). Probes of *cyp19a1* were transcribed from the clone of full-length medaka
248 *cyp19a1* cDNA (Fukada et al., 1996). The PCR primer sets amplified template DNA
249 for other genes were shown in Supplemental table 1. The gonads were fixed in 4%
250 paraformaldehyde in 0.85X phosphate-buffered saline (PBS) at 4 °C overnight. After
251 fixation and processing, tissues were embedded in paraffin and serial 5 µm sections
252 were cut. At least three specimens were prepared for each time point. For in situ
253 hybridization, sections were deparaffinized, hydrated, and treated with 4 µg/ml
254 proteinase K (Roche Diagnostics) at 37 °C for 5 min, and then hybridized with sense
255 or antisense DIG-labeled RNA probes at 60 °C for 24 hr. Hybridization signals were
256 then detected using alkaline phosphatase-conjugated anti-DIG antibody (Roche
257 Diagnostics) and NBT/BCIP (Roche Diagnostics) as chromogen according to a
258 previous protocol (Nakamoto et al., 2012). For two-color in situ hybridization,
259 fluorescein isothiocyanate (FITC)-labeled and DIG-labeled cRNA probes were used.
260 Detection of RNA probes was achieved using the TSA Plus Fluorescein / TMR
261 System (PerkinElmer. Inc., Waltham, MA). Sections were counterstained with DAPI
262 and mounted using Fluoromount (Diagnostic Bio Systems, Pleasanton, CA).

263

264 2.8. *RNAseq*

265 The ovaries were cut in half along the longitudinal axis. One half of each ovary
266 was fixed in Bouin's solution and processed, sectioned and stained as described
267 above in order to determine the morphological condition of ovaries and classify the

phase of sex reversal. The other ovary halves were stored in RNAlater (QIAGEN, Hilden, Germany) and total RNA extracted using an RNeasy Mini Kit (QIAGEN, Hilden, Germany). RNA was used to synthesize a sequencing library that was sequenced (single-end 36 bp reads) using Hiseq 2000 (Illumina, San Diego, CA) according to the standard protocols of the High Throughput Sequencing Center, University of Washington. The sequencing data was submitted to the DDBJ Sequence Read Archive (DRA) under accession number DRA005629. Raw reads were cleaned using SolexaQA to remove low-quality sequences (Cox et al., 2010). Low quality reads (error probability less than 0.05) and short read sequences (length below 25bp) were discarded. The trimmed reads were mapped to the medaka annotated reference genome sequences (Ensemble release 75) which annotated 25,434 transcripts using RSEM with default parameters (Li and Dewey, 2011; Cunningham et al., 2015). Mean size of contigs was 1,507.3 bp. Differential gene expression analysis was performed using the TCC package (Sun et al., 2013). Contigs (5,934) with average read counts of less than 10 were eliminated from the analysis. Normalization and detection were performed using the DEGES/edgeR pipeline in the TCC package. The significance level of differentially expressed transcripts was set at a false discovery rate (FDR) of less than 0.01. GO enrichment analysis of DEGs was performed using the g:profiler (Reimand et al., 2007, 2011). A total of 76.7% of reference transcripts were annotated by GO terms. The significance level of GO term enrichment was set at an FDR-adjusted p value of less than 0.05. Then, significantly enriched GO terms were clustered by Revigo to generate a treemap (Supek et al., 2011). In the treemap, related GO terms were joined into clusters, and visualized with different colors. Size of the rectangles was adjusted to reflect the p-value. The larger rectangles indicated higher significance.

3. Results

3.1. *Screening of cyp19a1 mutants medaka*

To determine the function of estrogens in differentiation and development of the ovary, we screened for *cyp19a1* (ovarian aromatase) mutant medaka from an N-ethyl-N-nitrosourea (ENU)-based gene-driven mutagenesis library distributed by the National Bioresource Project (NBRP) medaka, Japan (Taniguchi et al., 2006). The ENU-based gene-driven mutagenesis library of medaka contains genomic DNA and frozen sperm of 5,771 F_1 males. We sequenced the genomic region of *cyp19a1* and found two pre-mature stop mutants, *cyp19a1* (K164X) and *cyp19a1* (Q183X) (Fig. 1A). In the K164X strain, lysine in exon 3 (AAA) was mutated to the stop codon TAA (Fig. 1B). In the Q183X strain, glutamine in exon 4 (CAG) was altered to the stop codon TAG (Fig. 1C). In histological analysis, the K164X and Q183X strains displayed the same phenotype. Thus, we used the K164X strain for subsequent experiments, because we were able to genotype this strain by PCR-RFLP.

3.2. *Estrogen synthesis by cyp19a1 mutant*

In the *cyp19a1* deficient mutant, we assumed that the activity of ovarian aromatase would be lost and thus estrogen biosynthesis should be abolished or greatly reduced in the gonad. To investigate the steroidogenic activity of aromatase in *cyp19a1* mutant medaka, we measured the level of estradiol-17β in the ovaries of adult *cyp19a1* (K164X) strain at 3 months after hatching by RIA. In *cyp19a1* $(K164X)^{-/-}$ females, estradiol-17β was not detectable in the ovaries of three out of four fish. One fish had 16.9 pg / gonad (33.8 pg/ml extract), which is very close to detection limit of the assay (31 pg/ml extract). By contrast, a mean of 80.4±6.0 (S.E.) pg estradiol-17β / ovary was detected in *cyp19a1* $(K164X)^{+/-}$ ovaries (Table 1). To

318 investigate if the very low levels of estradiol-17β detected in ovary of *cyp19a1*
319 (K164X)$^{-/-}$ mutants were sufficient to have biological effects, we examined the
320 expression of vitellogenin mRNA in the adult liver by RT-PCR. In teleost fish,
321 estrogens (principally estradiol-17β) synthesized by ovaries highly up-regulate the
322 expression of vitellogenin mRNA in the liver (Scholz et al., 2004). In medaka, two
323 vitellogenin genes, vitellogenin1 (*vtg1*) and vitellogenin2 (*vtg2*) have been reported
324 (Tong et al., 2004). Both *vtg1* and *vtg2* transcripts were detected in the liver of
325 *cyp19a1* (K164X)$^{+/-}$ females, but were absent in the liver of *cyp19a1* (K164X)$^{-/-}$
326 mutants (Fig. 2). Thus, the minute amount of estrogens in ovaries of *cyp19a1*
327 (K164X)$^{-/-}$ females could not induce transcription of vitellogenin.
328 Because aromatase catalyzes the conversion of testosterone to estrogens, we
329 examined whether the reduction of aromatase activity would result in an increase
330 in testosterone. We measured the amount of testosterone in the *cyp19a1* (K164X)
331 strain by ELISA. A mean of 0.42±0.20 (S.E.) ng/gonad of testosterone was detected
332 in *cyp19a1* (K164X)$^{+/-}$ ovaries (n=4), whereas 0.35±0.08 ng/gonad of testosterone was
333 detected in *cyp19a1* (K164X)$^{-/-}$ ovaries (n=4) at 3 months after hatching, just after
334 heterozygous siblings started spawning. These values are not statistically different
335 (t-test, p=0.37). Thus, the amount of testosterone was not increased in ovaries of
336 *cyp19a1* mutants at 3 months after hatching.
337
338 3.3. *Gonadal development of cyp19a1 mutant*
339 To clarify the function of estrogens during gonadal differentiation and
340 development, we investigated the development of gonads in the *cyp19a1* (K164X)
341 mutants histologically. In medaka, oogenesis is initiated just after hatching
342 (Kanamori et al, 1985; Kobayashi et al., 2004). The expression of ovarian

343 steroidogenic enzymes is first detectable at five to ten days after hatching (Suzuki
344 et al., 2004; Nakamoto, et al., 2010, 2012). At ten days after hatching, the gonads of
345 genetic female (XX) *cyp19a1* (K164X)$^{-/-}$ mutants contained oocytes at the diplotene
346 stage (Supplemental Fig. 1A). At 20 days after hatching, ovaries of *cyp19a1*
347 (K164X)$^{-/-}$ mutants had developed normally (Supplemental Fig. 1C and E). The cell
348 masses that differentiate into the roof of the ovarian cavity were observed in
349 *cyp19a1* (K164X)$^{-/-}$ mutants (Supplemental Fig. 1C arrow). Ovarian cavities were
350 observed at 30 days after hatching in both mutants and heterozygous siblings
351 (Supplemental Fig. 1E and F). The ovarian cavity and oviduct were elongated
352 towards the genital pore (Supplemental Fig. 1G). In another *cyp19a1* mutant
353 (Q183X)$^{-/-}$ strain, gonads of XX individuals developed into ovaries of normal
354 appearance that contained many oocytes and an ovarian cavity at 30 dah
355 (Supplemental Fig. 2A). In medaka, spawning starts from 2.5 to 3 months after
356 hatching under suitable conditions. At 2 months after hatching, the ovaries of XX
357 *cyp19a1* (K164X)$^{-/-}$ mutants contained many oocytes (Fig. 3A'). Thereafter, the
358 morphology of the anal fin of XX *cyp19a1* (K164X)$^{-/-}$ mutants gradually changed
359 from 3 to 6 months after hatching to the male type (Fig. 3A-D). In medaka, the
360 typical male secondary sex characters are a notched dorsal fin, parallelogram-like
361 morphology of the anal fin, and papillary processes of the anal fin. At 6 months after
362 hatching, the anal fins of genetic female *cyp19a1* (K164X)$^{-/-}$ mutants were the
363 typical male type with papillary processes (Fig. 3D, white arrow). The ovaries of XX
364 *cyp19a1* (K164X)$^{-/-}$ mutants became large at 3 months after hatching (Fig. 3B'). XX
365 *cyp19a1* (K164X)$^{-/-}$ mutants did not spawn, although heterozygous female sibling
366 females spawned at 3 months after hatching. At 3.5 months after hatching, ovarian
367 follicles were located only in the ventral side of the ovary of XX *cyp19a1* (K164X)$^{-/-}$

368 mutants (Fig. 3C'). Ovarian follicles were not observed in the dorsal side of these
369 ovaries. By 6 months after hatching, these ovaries had degenerated and
370 well-developed ovarian follicles were absent (Fig. 3D'). By contrast, in XY *cyp19a1*
371 $(K164X)^{-/-}$ males, gonads differentiated into testes and developed normally. Adult
372 *cyp19a1* $(K164X)^{-/-}$ males were fertile (data not shown).
373
374 3.4. *Process of degeneration of the adult ovary of cyp19a1 mutants*
375 We then analyzed the process of degeneration of the adult ovary in *cyp19a1*
376 mutants histologically. At 2 months after hatching, just before sexual maturation,
377 ovaries of XX *cyp19a1* $(K164X)^{-/-}$ females appeared normal (Fig. 4A). The mean
378 diameter of the largest follicles was 397.2 ±24.4 (S.E.) μm (n=5). These ovarian
379 follicles were of a size considered to be vitellogenic according to stages of oocyte
380 development described in Iwamatsu et al. (1988). At 2.5 months after hatching,
381 when heterozygous siblings initiated spawning, many ovarian follicles in the
382 ovaries of *cyp19a1* $(K164X)^{-/-}$ females had developed to the vitellogenic size (Fig. 4B).
383 However, unlike the ovarian follicles of heterozygous fish, eosin Y-positive yolk was
384 not observed in these ovarian follicles (Fig. 4B and I). In addition, abnormal
385 proliferation of the granulosa cell layers of the ovarian follicles was observed in
386 ovaries of *cyp19a1* $(K164X)^{-/-}$ females, characterized by granulosa cell layers that
387 were thicker than seen in *cyp19a1* $(K164X)^{+/-}$ females. The mean diameter of these
388 abnormal follicles was 563.0±15.1 (S.E.) μm (n=4 fish, 5 ovarian follicles / fish), a
389 size equivalent to late vitellogenic stage follicles of heterozygous siblings.
390 Post-vitellogenic maturing follicles were not observed in the ovaries of *cyp19a1*
391 $(K164X)^{-/-}$ fish. In *cyp19a1* $(Q183X)^{-/-}$ ovaries, oocytes also grew to the vitellogenic
392 size but there was no accumulation of eosin Y positive yolk. Abnormal proliferation

393 of the granulosa cell layers of the ovarian follicles was also observed at 3 mah
394 (Supplemental Fig. 2B).

395 To further compare the ovarian follicles of *cyp19a1* (K164X)$^{+/-}$ females with
396 those of *cyp19a1* (K164X)$^{-/-}$ females, we analyzed the expression of granulosa cell
397 and theca cell markers by *in situ* hybridization. In *cyp19a1* (K164X)$^{+/-}$ females, a
398 critical gene for differentiation of granulosa cells, *foxl2* (winged helix/forkhead
399 transcription factor L2), was expressed in granulosa cells of both pre-vitellogenic
400 and vitellogenic ovarian follicles (Fig. 5G and I) (Nakamoto et al., 2006). In these
401 females, *cyp19a1* was mainly expressed in both granulosa cells and theca cells of
402 vitellogenic stage ovarian follicles (Fig. 5H and P) (Suzuki et al., 2004), and *cyp17-I*
403 (*cyp17a1*) was expressed in follicular cells of late vitellogenic follicles and
404 interstitial thecal cells (Fig. 5Q) (Zhou et al., 2007). In ovaries of *cyp19a1* (K164X)$^{-/-}$
405 medaka, *foxl2* mRNA was detected in both pre-vitellogenic ovarian follicles and in
406 the larger, yolkless follicles that had achieved a size associated with vitellogenic
407 follicles; these follicles had thickened granulosa cell layers at 2 months after
408 hatching (Fig. 5A). *Cyp19a1* mRNA in *cyp19a1* (K164X)$^{-/-}$ ovaries was mainly
409 detected in follicular cells (granulosa cells and thecal cells) of vitellogenic-sized
410 follicles (Fig. 5B, C and J). *Cyp19a1* was also expressed in the proliferated, thick
411 granulosa cell layer. *Cyp17-I* mRNA was detected in interstitial cells, but not in
412 granulosa cells.

413 At 3.5 months after hatching, the degeneration of ovarian tissues became
414 advanced in gonads of *cyp19a1* (K164X)$^{-/-}$ females (Fig. 4C and D). The number of
415 ovarian follicles decreased drastically and many collapsed ovarian follicles were
416 observed. Interstitial cells proliferated abnormally. To determine if the degeneration
417 of ovarian tissues was due to apoptotic signaling processes, we subjected sections to

418 the TUNEL (TdT-mediated dUTP nick end labeling) assay but did not detect any
419 signal characteristic of programmed cell death (data not shown). Moreover, tissue
420 apparently undergoing spermatogenesis was observed near the ovarian cavity (Fig.
421 4D, arrowheads). At this stage, the expression of *foxl2* mRNA was detected in
422 ovarian follicles and the remnants of degenerated follicles (Fig. 5D asterisk),
423 whereas *cyp19a1* mRNA was detected only in intact ovarian follicles and was not
424 detected in the remnants of degenerated follicles (Fig. 5E and F). The expression of
425 *cyp17-I* was detected in theca-interstitial cells in gonads of *cyp19a1* (K164X)$^{-/-}$
426 females at 3.5 months after hatching (Fig. 5N and O). *Cyp17-I* mRNA was also
427 detected in theca-interstitial cells around the degenerated follicles.
428 Thereafter, at 5 to 6 months after hatching, spermatogenesis was observed
429 across the entire gonad (Fig. 4E and F, Supplemental Fig. 2C), and few oocytes
430 remained in K164X$^{-/-}$ and Q183X$^{-/-}$ female gonads. Spermatogenesis proceeded to
431 completion and mature sperm were observed (Fig. 4F, arrow, Supplemental Fig. 2C).
432 To confirm the differentiation of testicular tissue in the ovary of *cyp19a1* (K164X)$^{-/-}$
433 medaka, we examined the expression of the Sertoli cell markers doublesex and
434 mab-3 related transcription factor 1 (*dmrt1*) and gonadal soma derived factor (*gsdf*)
435 and the meiosis marker synaptonemal complex protein 3 (*scp3*) (Kobayashi et al.,
436 2004; Iwai et al., 2006; Shibata et al., 2010). In medaka testis, the expression of
437 *dmrt1* and *gsdf* was mainly detected in the somatic cells surrounding
438 spermatogonia located in the peripheral region of the testis and in the epithelium of
439 the efferent duct located in the central region of the testis (Supplemental Fig. 3 G-I).
440 In medaka, spermatogenesis proceeds from the peripheral region, where
441 spermatogonia are located, to the central region (Grier, 1981; Kanamori et al., 1985).

442 At 6 months after hatching, testis tissue that expressed *dmrt1* and *gsdf* was spread
443 across the entire region of the gonads of *cyp19a1* (K164X)$^{-/-}$ individuals
444 (Supplemental Fig. 3 A-C). Spermatocytes that expressed meiosis marker *scp3* were
445 also found throughout these gonads (Supplemental Fig.3 D-F). We did not observe
446 efferent duct-like structures. Thus, Sertoli cells had differentiated in the ovary of
447 *cyp19a1* (K164X)$^{-/-}$ medaka but the testicular structure in the *cyp19a1* (K164X)$^{-/-}$
448 ovary was not organized like wild-type testis. We bred one male fish with two
449 female fish in 3L water tanks. Under this rearing condition, most genetic female
450 (XX) *cyp19a1* (K164X)$^{-/-}$ individuals underwent sex reversal (10/11 fish). However,
451 when the mutant medaka were bred at a higher density (approximately 10 fish in
452 3L water tanks), the ovaries degenerated, but spermatogenesis did not occur.
453 Next, we assessed the fertilizing capacity of sperm produced by the ovaries of
454 *cyp19a1* (K164X)$^{-/-}$ fish. Phase contrast observation of sperm suspended in Balanced
455 Salt Solution (Iwamatsu, 1983) showed that sperm from the ovary of *cyp19a1*
456 (K164X)$^{-/-}$ fish had motility comparable to that of normal sperm from the testis (Fig.
457 4G and H). The sperm of XX *cyp19a1* (K164X)$^{-/-}$ medaka were able to fertilize eggs
458 (fertilization rate was 63.4 % (26/41 eggs)). These sperm were viable after freezing
459 using a standard protocol (Aoki et al., 1997; Krone and Wittbrodt, 1997).
460
461 3.5. *The origin of testicular tissue in adult ovary of cyp19a1 mutant*
462 To further understand the process of sex reversal in adult ovaries of medaka
463 associated with estrogen deficiency, we examine the expression patterns of Sex
464 determining region Y-box 9a2 (*sox9a2 / sox9b*) and *gsdf* in the *cyp19a1* (K164X)
465 strain using in situ hybridization. In medaka, *sox9a2* is expressed in
466 undifferentiated supporting cells surrounding germline stem cells in the adult

ovary (Nakamura et al., 2010). *Gsdf* is a critical factor for male sex differentiation in many teleost fish and is most likely the direct downstream target of the product of the sex determining gene *dmy* in the medaka (Shibata et al., 2010). At 2 months after hatching, before the initiation of the degeneration of the ovary in *cyp19a1* (K164X)$^{-/-}$ individuals, *sox9a2* was detected in somatic cells adjacent to the ovarian cavity (Fig. 6A, arrow). *Olvas* is an ortholog of *vasa* / *ddx4* (DEAD-box helicase 4), a critical gene for development and differentiation of germ cells in many species (Shinomiya et al., 2000). As expected, *sox9a2*-positive supporting cells surrounded *olvas*-positive germ cells (Fig. 6D). As in the ovaries of *cyp19a1* (K164X)$^{+/-}$ females, the expression of *gsdf* was not detected in *sox9a2*-positive supporting cells in *cyp19a1* (K164X)$^{-/-}$ ovaries at 2 months after hatching (Fig. 6A-C and N-P). At 3.5 months after hatching when degeneration of ovarian follicles was initiated, strong expression of *gsdf* was detected in somatic cells surrounding germ cells located near the ovarian cavity in ovaries of *cyp19a1* (K164X)$^{-/-}$ fish (Fig. 6E and G). *Gsdf*-positive supporting cells co-expressed *sox9a2* (Fig. 6H-J). In adult wild type ovaries, the expression of *gsdf* was weakly detected in granulosa cell of ovarian follicles (Fig. 6F). *Gsdf* mRNA was not detected in somatic cells surrounding germline stem cells located in the dorsal side of wild type ovaries (Fig. 6F arrowheads). Thereafter, in *cyp19a1* (K164X)$^{-/-}$ ovaries that progressed to an advanced stage of sex reversal, testicular tissue expressed *sox9a2* and *gsdf* broadly in the dorsal side of the gonads (Fig. 6K-M). The expression of *sox9a2* and *gsdf* was not detected in degenerated follicles (Fig. 6K-M, asterisk).

To determine if granulosa cells trans-differentiated into Sertoli cells during sex reversal in the adult ovaries of *cyp19a1* (K164X)$^{-/-}$ fish, we compared the expression of the granulosa cell marker *foxl2* and the Sertoli cell marker *gsdf* in

cyp19a1 (K164X)$^{-/-}$ gonads by two-color in situ hybridization. Just after the initiation of sex reversal, expression of *foxl2* was detected in degenerated follicles, whereas *gsdf*-positive cells were detected in the dorsal side of the ovary near the ovarian cavity (Fig. 7A-C). The expression of *foxl2* and *gsdf* was not co-localized in *cyp19a1* (K164X)$^{-/-}$ gonads. In gonads that had progressed to a more advanced stage of sex reversal, testicular tissue, marked by *gsdf* expression, was located in the dorsal side of the ovary near the ovarian cavity. *Foxl2*-positive female supporting cells were located separately from the testis tissue. Thus, there is no evidence of trans-differentiation of granulosa cells into Sertoli cells in the adult ovary during sex reversal of estrogen-deficient females.

3.6. *Transcriptome analysis of the progression of degeneration of ovaries and sex reversal*

To identify the genes potentially involved in the process of degeneration and sex reversal of adult ovary in the ovarian aromatase mutant, we carried out RNAseq analysis and detected differentially expressed transcripts during the degeneration of the ovary. We used three sets of ovarian RNA samples for Illumina sequencing during the degeneration of ovaries in *cyp19a1* (K164X)$^{-/-}$ individuals. Phase 1 ovaries were sampled before degeneration of the ovary commenced (n=8); Phase 2 ovaries were those in which ovarian follicles were degenerating (thick granulosa cell layer), but the external phenotype (morphology of fin) was female-type (n=4); and Phase 3 ovaries contained degenerating ovarian follicles and the fish displayed a male external phenotype (n=4). After filtering 68,453,192 ± 6,124,041 (mean±S.E.) raw Illumina reads, 63,853,564 ± 5,699,332 (mean±S.E.) trimmed reads were used for the following downstream analyses. A mean of 64.4%

517 reads was mapped to the reference genome. The number of raw reads, trimmed
518 reads and mapped reads are shown in Supplementary table 2. Then, two pairwise
519 comparisons (Phase 1 vs 2 and Phase 2 vs 3) were performed to identify
520 differentially expressed genes (DEGs) during the degeneration of ovaries, using
521 TCC (36). In comparisons between Phase 1 ovaries and Phase 2 ovaries, 2,338 DEGs
522 were detected at a FDR <0.01 (Fig. 8A and Supplemental table 3): 2,055 genes were
523 up-regulated and 283 genes were down-regulated. Lists of the top 15 up- and
524 down-regulated genes based on FDR are shown in Tables 2 and 3. The most highly
525 up-regulated genes included *hsd17b7* (Ensembl Transcript ID:
526 ENSORLT00000018892, 17ß-hydroxysteroid dehydrogenase type 7) which encodes
527 a steroidogenic enzyme involved in cholesterol synthesis and estrogen synthesis
528 (Moeller and Adamski, 2009; Mindnich and Adamski, 2009; Saloniemi et al., 2012)
529 and *srd5a1* (ENSORLT00000017993, 3-oxo-5-alpha-steroid 4-dehydrogenase 1)
530 which catalyzes the conversion of testosterone to dihydrotestosterone (Martyniuk,
531 et al., 2013). The Gene Ontology functional enrichment analysis of the 2,338
532 differentially expressed genes comparing Phase 1 to Phase 2 *cyp19a1* (K164X)$^{-/-}$
533 ovaries identified a total of 28 statistically enriched GO terms (Fig. 8C). All
534 annotated GO terms of DEGs were shown in Supplemental table 3. Twenty-seven
535 GO terms were associated with the 2,055 up-regulated genes and one GO term was
536 associated with the 283 down-regulated genes. Then, we summarized and
537 visualized the GO terms in the Biological Process category using REVIGO (Supek et
538 al., 2011). In comparisons between Phase 1 ovaries and Phase 2 ovaries,
539 significantly enriched GO terms in the Biological Process category were clustered by
540 translation, electron transport chain, metabolism, biosynthesis, extracellular
541 matrix, constituent secretion and cell cycle (Fig. 8D). The most overrepresented

cluster was translation.

Comparison of Phase 2 ovaries with Phase 3 ovaries revealed 597 DEGs with an FDR < 0.01 (Fig. 8B and Supplemental table 4): 555 genes were up-regulated and 42 genes were down-regulated. The top 15 up- and down-regulated genes based on FDR are shown in Tables 4 and 5. The Gene Ontology functional enrichment analysis identified 13 statistically enriched GO terms in this sex reversal process (Fig. 8E), all associated with the 567 up-regulated genes. No statistically enriched GO terms were associated with the 43 down-regulated genes. All annotated GO terms of DEGs are shown in Supplemental table 4.

Next, we used the RNAseq data to analyze the gene expression profiles of transcripts of major steroidogenic enzymes and steroidogenesis-related factors during the degeneration of ovaries in *cyp19a1* (K164X)$^{-/-}$ medaka (Fig. 9). The expression of cyp19a1 (ENSORLT00000003689), *foxl2* (ENSORLT00000025059), *ad4bp/sf-1* (ENSORLT00000020643), *star* (ENSORLT00000015903), *cyp11a1* (ENSORLT00000009022), *hsd3b* (ENSORLT00000010781), *hsd11b3* (ENSORLT00000005735), *srd5a1* (ENSORLT00000017993) and *cyp17a2* / *cyp17-II* (ENSORLT00000002786) were up-regulated significantly in Phase 2 ovaries (degenerating ovarian follicle, with a female external phenotype) compared to Phase 1 ovaries (before degeneration of the ovary was initiated) and expression was maintained at the same level during Phase 3 (degeneration of ovarian follicles, external male phenotype) (Fig. 9A and C-J). Expression of *cyp19a2* (brain type aromatase, ENSORLT00000006986) was detected at a low background level throughout these phases (Fig.9B). *Cyp17a1* / *cyp17-I* (ENSORLT00000023960) transcripts statistically increased from Phase 1 to Phase 2 and from Phase 2 to Phase 3 (Fig. 9G). Within the *hsd17b* enzyme family, *hsd17b1*

(ENSORLT00000005207), *hsd17b3* (ENSORLT00000005354), *hsd17b4* (ENSORLT00000004429), *hsd17b7* (ENSORLT00000018892), *hsd17b8* (ENSORLT00000008218), *hsd17b10* (ENSORLT00000020908), *hsd17b12a* (ENSORLT00000001759), *hsd17b12b* (ENSORLT00000001234) and *hsd17b14* (ENSORLT00000001964) were annotated to medaka genome sequences (Ensemble release 75) (Cunningham et al., 2015). *Hsd17b1* is mainly expressed in ovaries and catalyzes the conversion of estrone to estradiol-17β. *Hsd17b3* is mainly expressed in testes and catalyzes the conversion of androstenedione to testosterone. *Hsd17b4, hsd17b8, hsd17b10* and *hsd17b14* are expressed in various tissues and are considered to be involved in the inactivation of androgens and estrogens and in the synthesis of fatty acids in mammals. *Hsd17b7* mainly acts in cholesterol metabolism, and catalyzes the conversion of zymosterone to zymosterol. *Hsd17b7* also catalyzes the conversion of estrone to estradiol-17β in mammals. *Hsd17b12* is involved in the synthesis of long-chain fatty acids in various tissues. *Hsd17b12* is able to reduce estrone to estradiol-17β (Mindnich et al., 2004; Meier et al., 2009; Moeller and Adamski, 2009; Mindnich and Adamski, 2009; Saloniemi et al., 2012). In ovaries of *cyp19a1* (K164X)$^{-/-}$ mutants, the expression of *hsd17b1*, *hsd17b4*, *hsd17b8*, *hsd17b10*, and *hsd17b12a* did not change during the degeneration of the ovary (Fig. 9K). The expression levels of *hsd17b3*, *hsd17b7* and *hsd17b12b* were up-regulated significantly in Phase 2 ovaries compared to Phase 1 ovaries and were maintained at the same levels during Phase 3 (Fig. 9K). Expression of *hsd17b14* was detected at a low background level throughout these phases (data not shown).

4. Discussion

4.1. *De novo synthesis of estrogens is not critical for early ovarian differentiation of medaka.*

In this study, we identified two mutant medaka strains (K164X and Q183X) with premature stops in the ovarian aromatase (*cyp19a1*) gene from an N-ethyl-N-nitrosourea-based gene-driven mutagenesis library and described the process of ovarian development, which appeared normal until the time of puberty in non-mutants. Histological analysis revealed that both *cyp19a1* mutant medaka strains showed the same phenotype, indicating that the phenotype of these medaka mutants is a consequence of a mutation of *cyp19a1* gene and not due to other various point mutations induced by ENU-based mutagenesis. The activity of ovarian aromatase was extremely reduced in *cyp19a1* (K164X) mutants, as evidenced by very low/non-detectable estradiol-17β levels compared those in heterozygous females, and the lack of evidence for expression of the estradiol-17β-regulated hepatic vitellogenin gene. We also explored the possibility that brain type aromatase *cyp19a2* / *cyp19b* might compensate for the loss of the aromatase activity in the ovary of the *cyp19a1* mutant. We isolated a premature stop *cyp19a2* mutant from the mutagenesis library in which lysine at position 105 (AAG) was mutated to the stop codon TAG (Supplemental figure 4). Preliminary histological analysis of the *cyp19a1* / *cyp19a2* double mutant gonads revealed the same morphological phenotype as those of the *cyp19a1* K164X$^{-/-}$ and Q183X$^{-/-}$ mutants (data not shown). Analysis of estrogen levels in developing ovaries of the *cyp19a1* / *cyp19a2* double mutant would further confirm these findings. Consequently, we might exclude the possibility that morphologically normal ovarian differentiation and early ovarian follicle development progressed in *cyp19a1*

(K164X)$^{-/-}$ mutant medaka because of the compensation by brain type aromatase for loss of aromatase activity encoded by the ovarian form.

In *cyp19a1* (K164X) mutants, the indifferent gonads first differentiated into ovaries according to genetic sex. Previous reports indicated that the first morphological signs of a sex difference in gonadal morphology between males and females occurred at stage 38 (one day before hatching) in medaka (Hamaguchi, 1982; Matsuda et al., 2002; Kobayashi et al., 2004). The expression of steroidogenic enzymes including *cyp19a1* was detected from five to ten days after hatching (Suzuki et al., 2004). Thus, the initiation of *cyp19a1* expression occurred well after the first appearance of a morphological sex difference in medaka. Oral administration of the aromatase inhibitor Fadrozole did not induce female-to-male sex reversal in medaka (Suzuki et al., 2004). These previous reports suggested that endogenous estrogens that are synthesized *de novo* after fertilization are not critical for early ovarian differentiation in medaka. The phenotype of the *cyp19a1* mutants is in agreement with the results of these previous reports. A recent study employing gene editing methods to knockout *cyp19a1a* in zebrafish showed that undifferentiated gonads differentiated first into ovaries containing early perinucleolar oocyte-like germ cells, but unlike medaka *cyp19a1* mutants, spermatogenesis was then rapidly initiated in all knockout fish (Lau et al., 2016). We conclude that estrogens that are synthesized after fertilization are also not critical determinants for the initiation of ovarian determination and differentiation in medaka. The process of gonadal differentiation varies between medaka and zebrafish: undifferentiated gonads directly differentiate into testes or ovaries in medaka while in zebrafish, irrespective of genetic sex, undifferentiated gonads first differentiate into ovaries and then sex reverse into testis in male zebrafish.

642 Although the process of gonadal differentiation is different in these species, in both
643 *de novo* synthesis of estrogens is not critical for early ovarian differentiation.
644 Conversely, endogenous estrogens have been generally considered to drive ovarian
645 differentiation in other teleost fish (Nakamura et al., 1998; Guiguen et al., 2010).
646 Recently, we found marked increases in the expression of estrogen receptor β2
647 (*ERβ2*), but not either *ERα* or *ERβ1*, in genetically female embryos of medaka
648 during sex differentiation. Furthermore, E_2 treatment induced marked
649 up-regulation of *ERβ2* expression in genetically male embryos (Chakraborty et al.,
650 2011). Paradoxically, increased *ERβ2* expression occurs far earlier in the ovarian
651 differentiation than the expression of aromatase and steroidogenic enzymes
652 developmental stage (Suzuki et al., 2004; Nakamoto et al., 2010; Chakraborty et al.,
653 2011). In medaka embryos, maternal estrogens accumulate in yolk during oogenesis
654 (Iwamatsu et al., 2005). Although concentrations of estrogens in the yolk of teleost
655 eggs very rapidly decrease after fertilization, low levels of maternal estrogens
656 remain in the yolk (Paitz et al., 2015). The question of whether low levels of
657 maternal estrogens in the yolk of medaka embryos would be sufficient to drive
658 ovarian differentiation via ERβ2 requires investigation.
659
660 4.2. *Other factors promote oocyte growth in estrogen-deficient medaka*
661 At 10 and 20 days after hatching, ovaries of genetic female *cyp19a1* (K164X)$^{-/-}$
662 mutants had developed normally and contained oocytes at the diplotene stage. The
663 number of oocytes in mutant and heterozygous siblings appeared to be similar.
664 Proliferation of oogonia and the onset of meiosis proceeded in the absence of
665 endogenous estrogens. In zebrafish, estrogens are not essential for proliferation of
666 oogonia and the onset of meiosis (Lau et al., 2016). In Japanese huchen and common

667 carp, estradiol-17β and the progestin, 17α,20β-dihydroxy-4-pregnen-3-one (DHP) are
668 involved in the very early phases of oocyte development. Estradiol-17β acts directly
669 to increase oogonial proliferation, as does DHP, which also can initiate the first
670 meiotic division (Miura et al., 2007). DHP could conceivably also regulate
671 proliferation of oogonia and onset of meiosis during early ovarian differentiation in
672 estrogen-deficient medaka. However, initial expression of the enzyme p450scc,
673 which catalyzes the first step in steroidogenesis (conversion of cholesterol to
674 pregnenolone), occurred after the onset of meiosis in medaka ovaries, suggesting
675 that synthesis of endogenous DHP did not occur during the period of proliferation of
676 oogonia and onset of meiosis (Nakamoto et al., 2010). Our results suggest that
677 oogonial proliferation and onset of meiosis are not regulated by estrogens and DHP
678 in medaka. The contrasting modes of ovarian development between these teleost
679 models may necessitate differences in the mechanisms regulating oogonial
680 proliferation and onset of meiosis. The Japanese huchen and common carp display
681 group-synchronous oocyte development, with only a single clutch of vitellogenic
682 (estradiol-17β–synthesizing) follicles present at any time in the adult ovary. E_2
683 levels are only elevated during vitellogenesis of a single clutch of oocytes. Medaka
684 and zebrafish are polytelic fish with asynchronous oocyte development, and ovaries
685 contain ovarian follicles at various stages of development. Because E_2 synthesizing
686 follicles are always present in medaka ovary, all oogonia and follicles would be
687 exposed to E_2, suggesting the existence of mechanisms for the protection of oogonia
688 and ovarian follicles at non-vitellogenic stages in teleost ovaries with asynchronous
689 oocyte development from E_2.

690 Ovaries of *cyp19a1* $(K164X)^{-/-}$ females displayed normal primary growth of
691 oocytes with development to the early cortical alveoli stage, which is considered to

692 mark the completion of primary growth (Lubzens et al., 2010; Kagawa, 2013),
693 suggesting that primary growth does not depend on estrogens. In some teleost,
694 androgens such as 11-ketotestosterone (11-KT) induce primary growth and
695 previtellogenic ovarian development (Lokman et al., 2007; Kortner et al., 2009;
696 Forsgren and Young, 2012). Thus, androgens might induce primary growth of
697 oocytes and synthesis of cortical alveoli in *cyp19a1* mutant medaka.

698 In ovaries of *cyp19a1* $(K164X)^{-/-}$ females, ovarian follicles developed to the size
699 of vitellogenic follicles in wild-type females, but without eosin Y-positive yolk.
700 Vitellogenin genes were not expressed in liver. In these vitellogenic-sized ovarian
701 follicles, *cyp19a1* mRNA transcripts were detected in the granulosa cell layer. In
702 wild-type medaka, *cyp19a1* is first expressed in theca cells of pre-vitellogenic
703 follicles and then in both theca cells and granulosa cells of vitellogenic follicles
704 (Nakamura et al., 2009). In teleost fish, FSH from pituitary regulates the
705 vitellogenic growth of ovarian follicles, partly through the stimulation of
706 estradiol-17β synthesis in ovarian follicles. Estrogens regulate growth of ovarian
707 follicles through stimulation of vitellogenin synthesis in the liver (Nagahama and
708 Yamashita, 2008; Lubzens et al., 2010). That mutant ovarian follicles develop to the
709 same size as wild-type follicles but without the accumulation of yolk suggests that
710 the growth of ovarian follicles and the incorporation of vitellogenin may be
711 uncoupled processes, with FSH potentially stimulating an increase in ovarian
712 follicle size in the absence of the stimulation of vitellogenin synthesis by estrogens.
713 Granulosa cells of ovarian follicles then proceeded to proliferate abnormally in
714 ovaries of *cyp19a1* mutants, resulting in granulosa cell layers that were thicker
715 than seen in heterozygous females. Transcriptome analysis indicated that the genes
716 functionally grouped under the process of translation are enriched at the time of

granulosa cell proliferation. These results suggest that protein synthesis was highly up-regulated during the abnormal proliferation of granulosa cells.

Apparently normal ovarian cavities were present in the developing ovaries of *cyp19a1* (K164X)$^{-/-}$ mutants. In other studies, oral administration of the selective aromatase inhibitor Fadrozole to medaka from 30 days after hatching inhibited the formation of the ovarian cavity but did not affect early oogenesis and folliculogenesis. However, brief treatment of XY larvae with E_2 induced an ovarian cavity-like structure in testis (Suzuki et al., 2004). These studies might be reconciled by differences in residual levels of estrogens. It is possible that oral administration of Fadrozole did not completely inhibit aromatase activity. The detailed downstream pathway induced by estrogens during ovarian cavity formation has not been determined. Unknown factors in this pathway might activate ovarian cavity formation at very low levels of estrogens during ovarian development of *cyp19a1* mutants.

Thereafter, ovarian follicles with thick granulosa cell layers began degenerating. At a time when heterozygous siblings were ovulating, the phenotype of the *cyp19a1* mutants indicated that estrogen-deficiency does not impact development of ovarian follicles up to the stage when wild-type follicles would enter vitellogenesis. Transcriptome analysis reveals that transcripts for most steroidogenic enzymes and steroidogenesis-related factors were up-regulated after ovarian follicles started showing the first signs of degeneration. It is possible that elevated levels of FSH resulting from a lack of negative feedback by estrogens on the hypothalamus and/or pituitary increased expression of these genes (Breton et al., 1997; Dickey and Swanson, 1998; Saligaut et al., 1998; Luckenbach et al., 2011). Our transcriptome analysis did not compare mutant and wild type ovaries because

742 oocytes in mutant ovaries did not accumulate yolk and we were concerned that the
743 vast quantities of mRNAs known to accumulate in yolk would not allow
744 identification of relatively scarce follicle cell transcripts. Thus, we are unable to
745 exclude the possibility that the identified up-regulation of steroidogenic enzymes
746 and steroidogenesis-related factors are part of the normal developmental process.
747 Further studies employing a much deeper sequencing approach and/or isolation of
748 granulosa cell and thecal cell layers for transcriptome analysis between mutant and
749 wild type are needed. *Cyp19a2* (brain type aromatase) transcripts were expressed at
750 a low background level throughout the degeneration process of ovaries, suggesting
751 that *cyp19a2* could not compensate for the reduced aromatase activity in ovaries of
752 *cyp19a1* mutants. One of the highest up-regulated genes was *srd5a1* which
753 catalyzes the conversion of testosterone to 5α-dihydrotestosterone (DHT),
754 suggesting that medaka ovarian follicles have the potential to synthesize DHT. In
755 some teleost fish, DHT can induce hepatic vitellogenin synthesis *in vitro* and also
756 can increase estradiol-17β production in the teleost ovary (Martyniuk et al., 2013).
757 Production of DHT may have increased in ovaries of *cyp19a1* mutants. However, the
758 lack of expression of either vitellogenin gene suggests that DHT does not participate
759 in regulating vitellogenin synthesis in *cyp19a1* mutants.

760 Secondary sex characters changed to male type gradually. Because aromatase
761 catalyzes the conversion of testosterone to estrogens, it is conceivable that the
762 reduction of aromatase activity could lead to elevated levels of testosterone that
763 promoted both the degeneration of ovaries and spermatogenesis. However,
764 testosterone levels did not differ between wild-type ovaries and mutant ovaries at
765 the time of the initial phase of degeneration of ovarian follicles and sex reversal.
766 During the initial phase of degeneration of ovarian follicles, *srd5a1*, *hsd11b* and

767 *hsd17bs* were up-regulated. These results raise the possibility that testosterone
768 may be converted to DHT and / or 11-KT, both bioactive non-aromatizable
769 androgens, with the result that elevated levels of these androgens could induce
770 changes in the morphology of fins. In teleosts (Leino et al., 2003; Berg et al., 2014)
771 and mammals (Billig et al., 1993; Hsueh et al., 1994; Kaipia and Hsueh, 1997),
772 androgens induce atresia of ovarian follicles. We suggest that the imbalance of
773 estrogens and androgens, especially the potential for an increase in
774 non-aromatizable androgens could be part of the mechanism that induced
775 degeneration of ovarian follicles in ovaries of *cyp19a1* mutants.

776 In *cyp19a1a* knockout zebrafish, undifferentiated gonads differentiated first
777 into ovaries containing early perinucleolar oocyte-like germ cells, oocyte-like germ
778 cells then disappear and spermatogenesis was then rapidly initiated in all knockout
779 fish (Lau et al., 2016). During testicular differentiation of zebrafish, oocyte-like
780 germ cells disappeared at early diplotene stage via apoptotic processes (Uchida et
781 al., 2002). Therefore, in *cyp19a1a* knockout zebrafish, the normal programmed cell
782 death pathway during testicular differentiation may be activated due to a deficiency
783 in estrogen signaling, leading to the ovary-like gonads differentiating into testis.
784 Conversely, in *cyp19a1* mutant medaka, ovarian follicles developed and grew to
785 sizes characteristic of vitellogenic follicles but without yolk, and then degenerated.
786 We did not detect any evidence of programmed cell death in degenerating ovarian
787 follicles in medaka. The difference in the degeneration process of ovarian tissue
788 between *cyp19a1* mutant medaka and zebrafish might reflect the differences
789 between these species in the normal gonadal development process.

790

791 4.3. *Estrogens are essential for the maintenance of ovarian differentiation in*

792 *medaka.*

793 After vitellogenesis failed to proceed and ovarian degeneration began in
794 *cyp19a1* mutant medaka, spermatogenesis was observed in parts of the degenerated
795 ovary. Our histological observations during the sex reversal process indicate that
796 ovarian tissues degenerated initially, followed by the differentiation of testicular
797 tissues from stem cells. RNAseq analysis indicated that levels of mRNAs for genes
798 related to the immune response were up-regulated during the sex reversal process
799 which might be expected during tissue remodeling. Immune cell markers are
800 expressed in the atretic follicles of mammals, and ovarian macrophages act to
801 remove cellular debris from atretic follicles (Takaya et al., 1997; Ruijin et al., 2004;
802 Hatzirodos et al., 2014a, 2014b). These up-regulated immune response genes may
803 function to promote atresia and to remove remnants of those follicles in mutant
804 medaka. Recent studies in female medaka and zebrafish showed that knockout of
805 the FSH receptor resulted in sex reversal (Murozumi et al., 2014; Zhang et al., 2015),
806 similar to the ovarian phenotype displayed by *cyp19a1* mutant medaka. In FSHR
807 mutant medaka, E2 levels in XX gonads were greatly reduced and some XX fish
808 contained testes. However, in our studies, we found evidence that spermatogenesis
809 is initiated from germline stem cells and *sox9a2*-positive (somatic) supporting cells.
810 Medaka is a daily spawning species and oogonia are continuously derived from
811 germline stem cells located in the dorsal side of ovaries (Nakamura et al., 2010).
812 Medaka germline stem cells and undifferentiated supporting cells in ovaries exhibit
813 sexual plasticity and differentiate into male type cells after treatment of adult
814 female medaka with an aromatase inhibitor (Paul-Prasanth et al., 2013). The
815 gonadal phenotype of *cyp19a1* mutants agrees well with those resulting from
816 treatment of adult medaka with aromatase inhibitors. *Foxl*3 (winged helix/forkhead

817 transcription factor L3) was expressed in germline stem cells, and controls
818 differentiation of germline stem cells to spermatogonia in this species (Nishimura et
819 al., 2015). *Sox9a2* is a HMG-box transcription factor and is expressed in supporting
820 cells of both sexes during early sexual differentiation of the indifferent gonads of
821 medaka (Nakamoto et al., 2005) and is critical for the proliferation and survival of
822 germ cells in both sexes (Nakamura et al., 2012). During the sex reversal process in
823 this study, *gsdf* was expressed in *sox9a2*-positive supporting cells. *Gsdf* encodes a
824 growth factor belonging to the TGF-β superfamily that is expressed in supporting
825 cells and regulates the proliferation of primordial germ cells and spermatogonia in
826 rainbow trout (Sawatari et al., 2007). Our results suggest that lack of estrogens in
827 medaka mutants leads to the differentiation of germline stem cells into
828 spermatogonia via actions on *sox9a2*- positive supporting cells. Gsdf secreted from
829 *sox9a2*-positive supporting cells might affect the mechanisms for cell fate
830 determination of germline stem cells regulated by *foxl3*. Estrogen deficiency and/or
831 imbalance in the ratio of estrogens and androgens may stimulate supporting cells to
832 differentiate into Sertoli cells. In turn, Sertoli cell-derived *gsdf* could induce the
833 differentiation of germline stem cells into spermatogonia (Fig. 10). In wild type
834 ovaries, estrogens maintain oogonia via the inhibitory action of *sox9a2* from
835 supporting cells on male differentiation. Under the steroid hormone environment
836 existing after puberty, *sox9a2*-positive supporting cells and germline stem cells
837 differentiate into *foxl2*-positive supporting cells (precursor of granulosa cells) and
838 oogonia, respectively. We provide direct evidence that estrogens maintain the
839 continuous differentiation of oogonia and granulosa cells from stem cells in adult
840 ovaries.

841 Knockout of aromatase or estrogen receptors in mice did not affect ovarian

842 differentiation and early follicle development but adults were either sterile or
843 severely subfertile (Fisher et al., 1998; Dupont et al., 2000). The phenotypes
844 associated with ovarian aromatase or estrogen-signaling deficiency are quite
845 similar between medaka and mouse; in both, estrogens are critical for maintenance
846 of ovarian differentiation in adults but are not essential for early ovarian
847 differentiation (Cutting et al., 2013). *Foxl2* / *Wnt4* pathway are critical for early
848 ovarian differentiation. Unlike mammals and medaka, estrogens are critical for
849 early ovarian differentiation in many teleost fish species (Nakamura et al., 1998;
850 Guiguen et al., 2010). It is not known if estrogen-independent ovarian
851 differentiation in vertebrates is an ancient mechanism subsequently lost in many
852 teleosts or one that arose independently in medaka (and presumably other
853 unstudied teleosts) and mammals.
854
855
856

Disclosure summary

The authors have no conflict of interest.

Acknowledgements

This work was supported by JSPS (The Japan Society for the Promotion of Science) Research Fellowships for Young Scientists (23-3821), and by Grant "The Young Researcher Overseas Visit Program for Accelerating Brain Circulation" from JSPS (G2213) which facilitated the long-term visits of MN and YS to the University of Washington. This work was partly supported by Grants-in-Aid for Young Scientists (B) (KAKENHI: 26840107) to MN. This work was also partially supported by National Science Foundation grant IOS-0949765 to GY and the National Institute for Basic Biology Priority Collaborative Research Project (12-105 and 13-103) to YT. The medaka strains were provided by the National Bioresource Project (NBRP) medaka, Japan. We thank Jon Dickey and Mollie Middleton (NOAA's Northwest Fisheries Science Center and University of Washington) for assaying estradiol-17β and testosterone levels. We appreciate Ms. Hiroe Ishikawa, Ms. Emiko Shibata, Ms. Chikako Takagi and Ms. Ikuyo Hara (National Institute for Basic Biology) for technical support.

878 ## References

879 Abramoff, M.D., Magalhaes, P.J., Ram, S.J. 2004. Image processing with ImageJ.
880 Biophot. Inter. 11, 36-42.

881 Aoki, K., Okamoto, M., Tatsumi, K., Ishikawa, Y. 1997. Cryopreservation of medaka
882 spermatozoa. Zool. Sci. 14, 641-644.

883 Billig, H., Furuta, I., Hsueh, A.J. 1993. Estrogens inhibit and androgens enhance
884 ovarian granulosa cell apoptosis. Endocrinology 133, 2204-2212.

885 Berg, A.H., Rice, C.D., Rahman, M.S., Dong, J., Thomas, P. 2014. Identification and
886 characterization of membrane androgen receptors in the ZIP9 zinc transporter
887 subfamily: I. Discovery in female atlantic croaker and evidence ZIP9 mediates
888 testosterone-induced apoptosis of ovarian follicle cells. Endocrinology 155,
889 4237-4249.

890 Breton, B., Sambroni, E., Govorun, M., Weil, C. 1997. Effects of steroids on GtH I
891 and GtH II secretion and pituitary concentration in the immature rainbow trout
892 Oncorhynchus mykiss. C. R. Acad. Sci. Paris 320, 783-789.

893 Chakraborty, T., Shibata, Y., Zhou, L.Y., Katsu, Y., Iguchi, T., Nagahama, Y. 2011.
894 Differential expression of three estrogen receptor subtype mRNAs in gonads and
895 liver from embryos to adults of the medaka, *Oryzias latipes*. Mol. Cell. Endocrinol.
896 333, 47-54.

897 Cox, M.P., Peterson, D.A., Biggs, P.J. 2010. SolexaQA: At-a-glance quality
898 assessment of Illumina second-generation sequencing data. BMC Bioinformatics 11,
899 485.

900 Cuisset, B., Pradelles, P., Kime, D.E., Kuhn, E.R., Babin, P., Le Menn, F. 1994.
901 Enzyme immunoassay for 11-ketotestosterone using acetylcholinesterase as label.
902 Application to the measurement of 11-ketotstosterone in plasma of Siberian

903 sturgeon. Comp. Biochem. Physiol. 108, 229-241.
904 Cunningham, F., Amode, M.R., Barrell, D., Beal, K., Billis, K., Brent, S.,
905 Carvalho-Silva, D., Clapham, P., Coates, G., Fitzgerald, S., Gil, L., Garcín Girón, C.,
906 Gordon, L., Hourlier, T., Hunt, S.E., Janacek, S.H., Johnson, N., Juettemann, T.,
907 Kähäri, A.K., Keenan, S., Martin, F.J., Maurel, T., McLaren, W., Murphy, D.N., Nag,
908 R., Overduin, B., Parker, A., Patricio, M., Perry, E., Pignatelli, M., Singh Riat, H.,
909 Sheppard, D., Taylor, K., Thormann, A., Vullo, A., Wilder, S.P., Zadissa, A., Aken,
910 B.L., Birney, E., Harrow, J., Kinsella, R., Muffato, M., Ruffier, M., Searle, S.M.J.,
911 Spudich, G., Trevanion, S.J., Yates, A., Zerbino, D.R., Flicek, P. 2015. Ensembl 2015.
912 Nucl. Acids Res. 43 (D1), D662-D669.
913 Cutting, A., Chue, J., Smith, C.A. 2013. Just How Conserved Is Vertebrate Sex
914 Determination? Dev. Dyn. 242, 380-387.
915 Dickey, J.T., Swanson, P. 1998. Effects of sex steroids on gonadotropin (FSH and
916 LH) regulation in coho salmon (*Oncorhynchus kisutch*). J. Mol. Endocrinol. 21,
917 291-306.
918 Dupont, S., Krust, A., Gansmuller, A., Dierich, A., Chambon, P., Mark, M. 2000.
919 Effect of single and compound knockouts of estrogen receptors α (ERα) and ß (ERß)
920 on mouse reproductive phenotypes. Development 127, 4277-4291.
921 Fisher, C.R., Graves, K.H., Parlow, A.F., Simpson, E.R. 1998. Characterization of
922 mice deficient in aromatase (ArKO) because of targeted disruption of the cyp19 gene.
923 Proc. Natl. Acad. Sci. USA 95, 6965-6970.
924 Forsgren, K.L., Young, G. 2012. Stage-specific effects of androgens and
925 estradiol-17beta on the development of late primary and early secondary ovarian
926 follicles of coho salmon (*Oncorhynchus kisutch*) *in vitro*. Biol. Reprod. 87, 64.
927 Fukada, S., Tanaka, M., Matsuyama, M., Kobayashi, D., Nagahama, Y. 1996.

928 Isolation, characterization, and expression of cDNAs encoding the medaka (*Oryzias*
929 *latipes*) ovarian follicle cytochrome P-450 aromatase. Mol. Reprod. Dev. 45, 285-290.
930 Grier, H.J. 1981. Cellular organization of the testis and spermatogenesis in fishes.
931 Amer. Zool. 21, 345-357.
932 Guiguen, Y., Fostier, A., Piferrer, F., Chang, C.F. 2010. Ovarian aromatase and
933 estrogens: a pivotal role for gonadal sex differentiation and sex change in fish. Gen.
934 Comp. Endocrinol. 165, 352-366.
935 Guzmán, J.M., Luckenbach, J.A., da Silva a, D.A.M., Ylitalo, G.M., Swanson, P.
936 2015. Development of approaches to induce puberty in cultured female sablefish
937 (*Anoplopoma fimbria*). Gen. Comp. Endocrinol. 221, 101-113.
938 Hamaguchi, S. 1982. A light- and electron-microscopic study on the migration of
939 primordial germ cells in the teleost, *Oryzias latipes*. Cell Tissue Res. 227, 139-151.
940 Hatzirodos, N., Hummitzsch, K., Irving-Rodgers, H.F., Harland, M.L., Morris, S.E.,
941 Rodgers, R.J. 2014a. Transcriptome profiling of granulosa cells from bovine ovarian
942 follicles during atresia. BMC Genomics 15, 40.
943 Hatzirodos, N., Irving-Rodgers, H.F., Hummitzsch, K., Rodgers, R.J. 2014b.
944 Transcriptome profiling of the theca interna from bovine ovarian follicles during
945 atresia. PLoS One 9, e99706.
946 Hsueh, A.J.W., Billig, H., Tsafriri, A. 1994. Ovarian follicle atresia: a hormonally
947 controlled apoptotic process. Endocr. Rev. 15, 707-724.
948 Iwai, T., Yoshii, A., Yokota, T., Sakai, C., Hori, H., Kanamori, A., Yamashita, M. 2006.
949 Structural components of the synaptonemal complex, SYCP1 and SYCP3, in the
950 medaka fish *Oryzias latipes*. Exp. Cell Res. 312, 2528-2537.
951 Iwamatsu, T. 1983. A new technique for dechorionation and observations on the
952 development of the naked egg in *Oryzias latipes*. J. Exp. Zool. 228, 83-89.

953 Iwamatsu, T., Ohta, T., Oshima, E., Sakai, N. 1988. Oogenesis in the medaka
954 *Oryzias latipes*: Stages of oocyte development. Zool. Sci. 5, 353-373.
955 Iwamatsu, T. 1994. Stages of normal development in the medaka *Oryzias latipes*.
956 Zool. Sci. 11, 825-839.
957 Iwamatsu, T. 1999. Convenient method for sex reversal in a freshwater teleost, the
958 medaka. J. Exp. Zool. 283, 210-214.
959 Iwamatsu, T., Kobayashi, H., Hamaguchi, S., Sagegami, R., Shuo, T. 2005.
960 Estradiol-17beta content in developing eggs and induced sex reversal of the medaka
961 (*Oryzias latipes*). J. Exp. Zool. A Comp. Exp. Biol. 303, 161-167.
962 Kagawa, H. 2013. Oogenesis in teleost fish. Aqua-BioScience Monographs 6, 99-127.
963 Lokman, P.M., George, K.A.N., Divers, S.L., Algie, M., Young, G. 2007.
964 11-Ketotestosterone and IGF-I increase the size of previtellogenic oocytes from
965 shortfinned eel, *Anguilla australis*, in vitro. Reprod. 133, 955-967.
966 Kanamori, A., Nagahama, Y., Egami, N. 1985. Development of the tissue
967 architecture in the gonads of the medaka *Oryzias latipes*. Zool. Sci. 2, 695-706.
968 Kaipia, A., Hsueh, A.J.W. 1997. Regulation of ovarian follicle atresia. Annu. Rev.
969 Physiol. 59, 349-363.
970 Kobayashi, T., Matsuda, M., Shibata, N., Suzuki, A., Nakamoto, M.,
971 Kajiura-Kobyashi, H., Nagahama, Y. 2004. Sex- and stage-specific expression of two
972 DM domain genes, DMY and DMRT1, during gonadal differentiation in the medaka,
973 *Oryzias latipes*. Dev. Dyn. 231, 518-526.
974 Korenman, S.G., Stevens, R.H., Carpenter, L.A., Robb, M., Niswender, G.D.,
975 Sherman, B.M. 1974. Estradiol radioimmunoassay without chromatography:
976 procedure, validation and normal values. J. Clin. Endocrinol. Metab. 38, 718–20.
977 Kortner, T.M., Rocha, E., Arukwe, A. 2009. Previtellogenic oocyte growth and

978 transcriptional changes of steroidogenic enzyme genes in immature female Atlantic
979 cod (*Gadus morhua* L.) after exposure to the androgens 11- ketotestosterone and
980 testosterone. Comp. Biochem. Physiol. A 152, 304-313.
981 Krone, A., Wittbrodt, J. 1997. A simple and reliable protocol for cryopreservation of
982 Medaka (*Oryzias latipes*) spermatozoa. Fish Biol. J. Medaka 9, 47-48.
983 Lau, E.S.W., Zhang, Z., Qin, M., Ge, W. 2016. Knockout of zebrafish ovarian
984 aromatase gene (*cyp19a1a*) by TALEN and CRISPR/Cas9 leads to all-male offspring
985 due to failed ovarian differentiation. Sci. Rep. 6, 37357.
986 Leino, R.L., Jensen, K.M., Ankley, G.T. 2005. Gonadal histology and characteristic
987 histopathology associated with endocrine disruption in the adult fathead minnow
988 (*Pimephales promelas*). Environ. Toxicol. Pharmacol. 19, 85-98.
989 Li, B., Dewey, N.C. 2011. RSEM: accurate transcript quantification from RNA-Seq
990 data with or without a reference genome. BMC Bioinformatics 12, 323.
991 Lubzens, E., Young, G., Bobe, J., Cerdà, J. 2010. Oogenesis in teleosts: how fish eggs
992 are formed. Gen. Comp. Endocrinol. 165, 367-389.
993 Luckenbach, J.A., Dickey, J.T., Swanson, P. 2011. Follicle-stimulating hormone
994 regulation of ovarian transcripts for steroidogenesis-related proteins and cell
995 survival, growth and differentiation factors in vitro during early secondary oocyte
996 growth in coho salmon. Gen. Comp. Endocrinol. 171, 52-63.
997 Martyniuk, C.J., Bissegger, S., Langlois, V.S. 2013. Current perspectives on the
998 androgen 5 alpha-dihydrotestosterone (DHT) and 5 alpha-reductases in teleost
999 fishes and amphibians. Gen. Comp. Endocrinol. 194, 264-274.
1000 Matsuda, M., Nagahama, Y., Shinomiya, A., Sato, T., Matsuda, C., Kobayashi, T.,
1001 Morrey, C.E., Shibata, N., Asakawa, S., Shimizu, N., Hori, H., Hamaguchi, S.,
1002 Sakaizumi, M. 2002. DMY is a Y-specific DM-domain gene required for male

1003 development in the medaka fish. Nature 417, 559-563.
1004 Meier, M., Möller, G., Adamski, J. 2009. Perspectives in understanding the role of
1005 human 17β-hydroxysteroid dehydrogenases in health and disease. Annals of the
1006 New York Academy of Sciences 1155, 15-24.
1007 Mindnich, R., Möller, G., Adamski, J. 2004. The role of 17β-hydroxysteroid
1008 dehydrogenases. Mol. Cell. Endocrinol. 218, 7-20.
1009 Mindnich, R., Adamski, J. 2009. Zebrafish 17beta-hydroxysteroid dehydrogenases:
1010 An evolutionary perspective. Mol. Cell Endocrinol. 301, 20-26.
1011 Miura, C., Higashino, T., Miura, T. 2007. A progestin and an estrogen regulate early
1012 stages of oogenesis in fish. Biol. Reprod. 77, 822-828.
1013 Moeller, G., Adamski, J. 2009. Integrated view on 17β-hydroxysteroid
1014 dehydrogenases. Mol. Cell. Endocrinol. 301, 7-19.
1015 Murozumi, N., Nakashima, R., Hirai, T., Kamei, Y., Ishikawa-Fujiwara, T., Todo, T.,
1016 Kitano, T. 2014. Loss of follicle-stimulating hormone receptor function causes
1017 masculinization and suppression of ovarian development in genetically female
1018 medaka. Endocrinology 155, 3136-3145.
1019 Nagahama, Y., Yamashita, M. 2008. Regulation of oocyte maturation in fish. Dev.
1020 Growth Differ. 50, 195-219.
1021 Nakamoto, M., Suzuki, A., Matsuda, M., Nagahama, Y., Shibata, N. 2005. Testicular
1022 type Sox9 is not involved in sex determination but might be in the development of
1023 testicular structures in the medaka, *Oryzias latipes*. Biochem. Biophys. Res.
1024 Commun. 333, 729-736.
1025 Nakamoto, M., Matsuda, M., Wang, D.S., Nagahama, Y., Shibata, N. 2006.
1026 Molecular cloning and analysis of gonadal expression of Foxl2 in the medaka,
1027 *Oryzias latipes*. Biochem. Biophys. Res. Commun. 344, 353-361.

1028 Nakamoto, M., Fukasawa, M., Orii, S., Shimamori, K., Maeda, T., Suzuki, A.,
1029 Matsuda, M., Kobayashi, T., Nagahama, Y., Shibata, N. 2010. Cloning and
1030 expression of medaka cholesterol side chain cleavage cytochrome P450 during
1031 gonadal development. Dev. Growth Differ. 52, 385-395.
1032 Nakamoto, M., Fukasawa, M., Tanaka, S., Shimamori, K., Suzuki, A., Matsuda, M.,
1033 Kobayashi, T., Nagahama, Y., Shibata, N. 2012. Expression of 3ß-hydroxysteroid
1034 dehydrogenase (hsd3b), star and ad4bp/sf-1 during gonadal development in medaka
1035 (*Oryzias latipes*). Gen. Comp. Endocrinol. 176, 222-230.
1036 Nakamura, M., Kobayashi, T., Chang, X.T., Nagahama, Y. 1998. Gonadal sex
1037 differentiation in teleost fish. J. Exp. Zool. 281, 362-372.
1038 Nakamura, M., Bhandari, R.K., Higa, M. 2003. The role estrogens play in sex
1039 differentiation and sex changes of fish. Fish Physiol. Biochem. 28, 113-117.
1040 Nakamura, S., Kurokawa, H., Asakawa, S., Shimizu, N., Tanaka, M. 2009. Two
1041 distinct types of theca cells in the medaka gonad: germ cell-dependent maintenance
1042 of *cyp19a1*-expressing theca cells. Dev. Dyn. 238, 2652-2657.
1043 Nakamura, S., Kobayashi, K., Nishimura, T., Higashijima, S., Tanaka, M. 2010.
1044 Identification of germline stem cells in the ovary of the teleost medaka. Science 328,
1045 1561-1563.
1046 Nakamura, S., Watakabe, I., Nishimura, T., Toyoda, A., Taniguchi, Y., Tanaka, M.
1047 2012. Analysis of medaka sox9 orthologue reveals a conserved role in germ cell
1048 maintenance. PLoS One 7, e29982.
1049 Nanda, I., Kondo, M., Hornung, U., Asakawa, S., Winkler, C., Shimizu, A., Shan, Z.,
1050 Haaf, T., Shimizu, N., Shima, A., Schmid, M., Schartl, M. 2002. A duplicated copy of
1051 DMRT1 in the sex-determining region of the Y chromosome of the medaka, *Oryzias*
1052 *latipes*. Proc. Natl. Acad. Sci. USA 99, 11778-117883.

1053 Nishimura, T., Sato, T., Yamamoto, Y., Watakabe, I., Ohkawa, Y., Suyama, M.,
1054 Kobayashi, S., Tanaka, M. 2015. Sex determination. *foxl3* is a germ cell-intrinsic
1055 factor involved in sperm-egg fate decision in medaka. Science 349, 328-331.
1056 Paitz, R.T., Mommer, B.C., Suhr, E., Bell, A.M. 2015. Changes in the concentrations
1057 of four maternal steroids during embryonic development in the threespined
1058 stickleback (*Gasterosteus aculeatus*). J. Exp. Zool. 323A, 422-429.
1059 Paul-Prasanth, B., Bhandari, B.K., Kobayashi, T., Horiguchi, R., Kobayashi, Y.,
1060 Nakamoto. M., Shibata, Y., Sakai, F., Nakamura, M., Nagahama, Y. 2013. Estrogen
1061 oversees the maintenance of the female genetic program in terminally
1062 differentiated gonochorists. Sci. Rep. 3, 2862.
1063 Reimand, J., Kull, M., Peterson, H., Hansen, J., Vilo, J. 2007. g:Profiler -- a
1064 web-based toolset for functional profiling of gene lists from large-scale experiments.
1065 Nucl. Acids Res. 35, 193-200.
1066 Reimand, J., Arak, T., Vilo, J. 2011. g:Profiler - a web server for functional
1067 interpretation of gene lists (2011 update). Nucl. Acids Res. 39, 307-315.
1068 Ruijin, W., Van der Hoek, K.H., Ryan, N.K., Norman, R.J., Robker, R.L. 2004.
1069 Macrophage contributions to ovarian function. Hum. Reprod. Update 10, 119-133.
1070 Saligaut, C., Linard, B., Mananos, E.L., Kah, O., Breton, B., Govoroum, M. 1998.
1071 Release of pituitary GtH I and GtH II in the rainbow trout (*Oncorhynchus mykiss*)
1072 at the beginning of vitellogenesis. Gen. Comp. Endocrinol. 109, 302-309.
1073 Saloniemi, T., Jokela, H., Strauss, L., Pakarinen, P., Poutanen, M. 2012. The
1074 diversity of sex steroid action: novel functions of hydroxysteroid (17β)
1075 dehydrogenases as revealed by genetically modified mouse models. J. Endocrinol.
1076 212, 27-40.
1077 Satoh, N., Egami, N. 1972. Sex differentiation of germ cells in the teleost, *Oryzias*

latipes, during normal embryonic development. J. Embryol. Exp. Morphol. 28, 385-395.

Sawatari, E., Shikina, S., Takeuchi, T., Yoshizaki, G. 2007. A novel transforming growth factor-b superfamily member expressed in gonadal somatic cells enhances primordial germ cell and spermatogonial proliferation in rainbow trout (*Oncorhynchus mykiss*). Dev. Biol. 301, 266-275.

Schneider, C.A., Rasband, W.S., Eliceiri, K.W. 2012. NIH Image to ImageJ: 25 years of image analysis. Nature Methods 9, 671-675.

Scholz, S., Kordes, C., Hamann, J., Gutzeit, H.O. 2004. Induction of vitellogenin in vivo and in vitro in the model teleost medaka (*Oryzias latipes*): comparison of gene expression and protein levels. Mar. Environ. Res. 57, 235-244.

Shibata, Y., Paul-Prasanth, B., Suzuki, A., Usami, T., Nakamoto, M., Matsuda, M., Nagahama, Y. 2010. Expression of gonadal soma derived factor (GSDF) is spatially and temporally correlated with early testicular differentiation in medaka, Gene Expr. Patterns 10, 283-289.

Shinomiya, A., Tanaka, M., Kobayashi, T., Nagahama, Y., Hamaguchi, S. 2000. The vasa-like gene, olvas, identifies the migration path of primordial germ cells during embryonic body formation stage in the medaka, *Oryzias latipes*. Dev. Growth Differ. 42, 317-326.

Shinomiya, A., Otake, H., Togashi, K., Hamaguchi, S., Sakaizumi, M. 2004. Field survey of sex-reversals in the medaka, *Oryzias latipes*: genotypic sexing of wild populations. Zool. Sci. 21, 613-619.

Sower, S.A., Schreck, C.B. 1982. Steroid and thyroid hormones during sexual maturation of coho salmon (*Oncorhynchus kisutch*) in seawater or fresh water. Gen. Comp. Endocrinol. 47, 42-53.

1103 Sun J, Nishiyama T, Shimizu K, Kadota K. 2013. TCC: an R package for comparing
1104 tag count data with robust normalization strategies. BMC Bioinformatics 14, 219.
1105 Supek, F., Bošnjak, M., Škunca, N., Šmuc, T. 2011. REVIGO summarizes and
1106 visualizes long lists of Gene Ontology terms. PLoS One 6, e21800.
1107 Suzuki, A., Tanaka, M., Shibata, N., Nagahama, Y. 2004. Expression of aromatase
1108 mRNA and effects of aromatase inhibitor during ovarian development in the
1109 medaka, *Oryzias latipes*. J. Exp. Zool. A Comp. Exp. Biol. 301, 266-273.
1110 Suzuki, A., Nakamoto, M., Kato, Y., Shibata, N. 2005. Effects of estradiol-17β on
1111 germ cell proliferation and DMY expression during early sexual differentiation of
1112 the medaka *Oryzias latipes*. Zool. Sci. 22, 791-796.
1113 Takatsu, K., Miyaoku, K., Roy, S.R., Murono, Y., Sago, T., Itagaki, H., Nakamura, M.,
1114 Tokumoto, T. 2013. Induction of female-to-male sex change in adult zebrafish by
1115 aromatase inhibitor treatment. Sci. Rep. 3, 3400.
1116 Takaya, R., Fukaya, T., Sasano, H., Suzuki, T., Tamura, M., Yajima, A. 1997.
1117 Macrophages in normal cycling human ovaries; immunohistochemical localization
1118 and characterization. Human Reprod. 12, 1508-1512.
1119 Taniguchi, Y., Takeda, S., Furutani-Seiki, M., Kamei, Y., Todo, T., Sasado, T.,
1120 Deguchi, T., Kondoh, H., Mudde, J., Yamazoe, H., Hidaka, M., Mitani, H., Toyoda, A.,
1121 Sakaki, Y., Plasterk, R.H.A., Cuppen, E. 2006. Generation of medaka gene knockout
1122 models by target-selected mutagenesis. Genome Biol. 7, R116.
1123 Tong, Y., Shan, T., Poh, Y.K., Yan, T., Wang, H., Lam, S.H., Gong, Z. 2004. Molecular
1124 cloning of zebrafish and medaka vitellogenin genes and comparison of their
1125 expression in response to 17β-estradiol. Gene. 328, 25-36.
1126 Uchida, D., Yamashita, M., Kitano, T., Iguchi, T. 2002. Oocyte apoptosis during the
1127 transition from ovary-like tissue to testes during sex differentiation of juvenile

zebrafish. J. Exp. Biol. 205, 711- 718.

Yamamoto, T. 1953. Artificially induced sex-reversal in genotypic males of the medaka (*Oryzias latipes*). J. Exp. Zool. 123, 571-594.

Yamamoto, T. 1959. A further study on induction of functional sex reversal in genotypic males of the medaka (*Oryzias latipes*) and progenies of sex reversals. Genetics 44, 739-757.

Yamamoto, T. 1969. Sex differentiation. In: Hoar WS, Randall DJ (eds) Fish Physiology. Academic Press, New York. pp117-175.

Young, G., Lokman, P.M., Kusakabe, M., Nakamura, I., Goetz, F.W. 2005. Gonadal steroidogenesis in teleost fish. In: *Molecular Aspects of Fish and Marine Biology* (C. Hew series ed.), *volume* 2 (N. Sherwood and P. Melamed, eds), World Scientific Press, Singapore. pp155-223.

Zhang, Z., Lau, S.W., Zhang, L., Ge, W. 2015. Disruption of zebrafish follicle-stimulating hormone receptor (fshr) but not luteinizing hormone receptor (lhcgr) gene by TALEN leads to failed follicle activation in females followed by sexual reversal to males. Endocrinology 156, 3747-3762.

Zhou, L.Y., Wang, D.S., Shibata, Y., Paul-Prasanth, B., Suzuki, A., Nagahama, Y. 2007. Characterization, expression and transcriptional regulation of P450c17-I and -II in the medaka, *Oryzias latipes*. Biochem. Biophys. Res. Commun. 362, 619-625.

Figure legends

Figure 1

Ovarian aromatase mutations. (A) Two pre-mature stop mutations were found: K164X located in exon3 and Q183X located in exon4. The arrowhead shows the mutated position. (B) The heterozygous individual (arom + / K164X) showed a double peak of adenine and thymine. (C) The heterozygous individual (arom + / Q183X) showed a double peak of cytosine and thymine.

Figure 2

Expression of vitellogenin in adult liver of ovarian aromatase mutants. RT-PCR analysis for vitellogenin1 (*vtg1*) and vitellogenin2 (*vtg2*) mRNA in adult liver. β-actin was used as an internal control. *Vtg1* and *vtg2* transcripts were not detected in adult liver of *cyp19a1* (K164X) strain (*cyp19a1*$^{-/-}$), while expression of these genes was detected in adult liver of heterozygous individuals (*cyp19a1*$^{+/-}$).

Figure 3

The gross morphology of anal fins and gonads in ovarian aromatase mutants (*cyp19a1* (K164X)). Micrographs at 2 months after hatching (mah) (A), 3 mah (B), 3.5 mah (C) and 6mah (D) are shown. Genetic female (XX) ovarian aromatase mutant medaka developed into females displaying ovaries (A and A'). Thereafter, the morphology of anal fins gradually changed into the male type (B-D). White arrows indicate papillary processes that are a typical male secondary sex character. At 3 months after hatch (mah), ovaries contained many oocytes (B'). At 3.5 mah, oocytes were located only in the ventral side of ovaries (C'). At 6 mah, ovaries degenerated and well-developed ovarian follicles were absent (Fig.3D'). Scale bars: 1

1178 mm.

1179

1180 Figure 4

1181 Histological analysis of the sex reversal process of ovarian aromatase mutant
1182 medaka. Tissue sections stained with hematoxylin-eosin are shown. The gonads of
1183 the *cyp19a1* (K164X) strain ($K164X^{-/-}$) at 2 months after hatching (mah) (A), 2.5 mah
1184 (B), 3.5 mah (C) and 5 mah (E) are shown. (D) High magnification image of the area
1185 marked with a rectangle in C. (F) High magnification image of the area marked
1186 with a rectangle in E. (I) The gonad of a heterozygous fish ($K164X^{+/-}$) at 3 mah is
1187 shown as control. The gonads of ovarian aromatase mutant XX medaka developed
1188 into ovaries according to genetic sex. (A) At 2 mah, the ovary appeared normal. (B)
1189 At 2.5 mah, oocyte growth proceeded. However, there was no accumulation of eosin
1190 Y positive yolk (Asterisk in I). Abnormal proliferation of granulosa cell layers was
1191 observed, manifested as granulosa cell layers that were much thicker than found in
1192 the *cyp19a1*$^{+/-}$ ovary (B and I). (C) At 3.5 mah, ovarian follicles degenerated. In parts
1193 of these gonads, spermatogenic-like tissue was observed (D, arrowheads). (E) At 5
1194 mah, spermatogenesis was observed throughout these gonads, with mature sperm
1195 present (F, arrow). Phase contrast image of sperm from an XX sex reversed male
1196 *cyp19a1* mutant medaka (G) and an XY male (H). In gonads of XX sex reversed
1197 male, functional sperm were present (arrows).. Scale bars: 100 μm in A-C, E and I,
1198 10 μm in D, F, G and H.

1199

1200 Figure 5

1201 Gene expression during the development of ovarian follicles of ovarian aromatase
1202 mutant medaka. (A- I) Double in situ hybridization for *foxl2* (red) and ovarian

aromatase (*cyp19a1*, green) at 2 months after hatching (mah) (A-C) and 3.5 mah in the XX *Cyp19a1* (K164X)$^{-/-}$ gonad (D-E), and in the *Cyp19a1* (K164X)$^{+/-}$ adult ovary (G-I). *Foxl2* (A, D, G), *cyp19a1* (B, E, H) and merged images (C, F, I) are shown. (J-R) Double *in situ* hybridization for *cyp19a1* (red) and *cyp17-I* (green) at 2 (J-L) and 3.5 mah (M-O) in the XX aromatase $^{-/-}$ gonad, and in the aromatase $^{+/-}$ adult ovary (P-R). *cyp19a1* (J, M, P), *cyp17-I* (K, N, Q) and merged images (L, O, R) are shown. *Foxl2* mRNA was detected continuously in granulosa cells of pre-vitellogenic follicles, vitellogenic follicles and in the remnants of degenerated follicles (D, asterisk). *Cyp19a1* mRNA was detected in granulosa cells of vitellogenic follicles, but not detected in the remnants of degenerated follicles (E and F, asterisk). In the ovary of ovarian aromatase mutants, expression of *cyp17-I* was mainly detected in interstitial cells (J-O). Follicles expressing *cyp17-I* in granulosa cells were not observed. In the ovary of heterozygous medaka, *cyp17-I* was expressed in both granulosa cells and interstitial cells (P-R). Sections were counterstained with DAPI in merged images. Scale bars: 100 μm.

Figure 6

Cell lineage of testis tissues in ovary of aromatase mutant medaka. Two color *in situ* hybridization for *sox9a2* / *sox9b* (red) and *gsdf* (green) in XX *cyp19a1* (K164X)$^{-/-}$ gonads at 2 months after hatching (mah) (A-C), and at 3.5 mah (H-J and K-M), and *cyp19a1* (K164X)$^{+/-}$ adult ovary (N-P). *sox9a2* (A, H, K and N), *gsdf* (B, I, L and O) and merged images (C, J, M and P) are shown. (D) Two color *in situ* hybridization for *sox9a2* (red) and the germ cell marker *olvas* (green) in the gonad 2 mah XX *cyp19a1*$^{-/-}$. *In situ* hybridization for *gsdf* in XX arom$^{-/-}$ gonads at 3.5 mah (E) and the adult *cyp19a1*$^{+/-}$ gonad (F). (G) Two color in situ hybridization for *gsdf* (red) and

olvas (green) in the XX *cyp19a1*$^{-/-}$ gonad at 3.5 mah. In medaka, germ line stem cells are surrounded by *sox9a2* -positive somatic cells (A-D, arrows). Weak expression of *gsdf* was detected in granulosa cells of pre-vitellogenic follicles (F). In the *cyp19a1*$^{-/-}$ ovary at 3.5 mah, strong expression of *gsdf* was also detected in somatic cells surrounding oogonia (E, arrowheads). In the arom$^{+/-}$ ovary and the *cyp19a1*$^{-/-}$ ovary before initiation of sex reversal, *sox9a2*-positive cells did not express *gsdf* (A-C, N-P, arrows). Thereafter, the *sox9a2*-positive somatic cells co-expressed *gsdf* in the *cyp19a1*$^{-/-}$ ovary at 3.5 mah (H-J, arrows). In the *cyp19a1*$^{-/-}$ ovary which progressed to an advanced stage of sex reversal, testis tissue expressing *sox9a2* and *gsdf* was located in the dorsal side of the gonads (K-M). The expression of *sox9a2* and *gsdf* was not detected in degenerated follicles (K-M, asterisk). Sections were counterstained with DAPI. Scale bars: 10 μm in A-J and N-P and 100 μm in K-M.

Figure 7

Cell lineage of testis tissues in ovary of aromatase mutant medaka. Double i*n situ* hybridization for *foxl2* (red) and *gsdf* (green) in XX *cyp19a1*$^{-/-}$ gonads. *Foxl2* (A, D), *gsdf* (B, E) and merged images (C, F) are shown. Gonads in the early phase of sex reversal (A-C), and in a more advanced stage of sex reversal (D-F) are shown. Testis tissues expressing *gsdf* were located in the dorsal side of ovary near the ovarian cavity. *Foxl2*-positive granulosa cells were located outside of the testis tissues. Sections were counterstained with DAPI. Scale bars: 100 μm.

Figure 8

Transcriptome analysis during the process of degeneration and sex reversal of ovary in ovarian *cyp19a1*mutants. (A) MA plot (a plot of fold change (M value) versus

base mean normalized counts (A value)) for comparison of ovary RNA samples before initiation of degeneration of ovary (phase 1), and after the commencement of degeneration of the ovarian follicle (thick granulosa cell layer) when the external phenotype (morphology of fin) was of the female type (phase 2). (B) MA plot for comparison of phase 2 mRNA samples with and samples in which ovarian follicles were degenerating and and external phenotype (fin shape) had changed to the male type (phase 3). The Y axis is the $\log_2$ fold change in the two samples. The X axis is the average $\log_2$ normalized counts in the two samples. Magenta points indicate the transcripts that are significantly different, identified by TCC at FDR < 0.01. A total of 2,338 differentially expression genes (DEG) were detected in phase 1 vs phase 2, and 597 DEG were detected in phase 2 vs phase 3. (C, E) Functional enrichment analysis of GO terms for DEG comparing phase 1 and phase 2 (C), and comparing phase 2 and phase 3 (E). GO enrichment analysis of DEG was performed using the g:profiler. The significance level of GO term enrichment was set at a FDR-adjusted p value less than 0.05. The X axis indicates $-\log_2$ (p-value). Black bars indicate significantly enriched GO terms in up-regulated genes. The gray bars indicate significantly enriched GO term in down-regulated genes. (D) The treemap (REVIGO) analysis for the summary of GO terms in biological processes for DEGs when comparing phase 1 and phase 2. In the treemap, related GO terms were joined into clusters and are visualized with different colors. Size of the rectangles was adjusted to reflect the p-value. The larger rectangles indicated higher significance.

Figure 9

Expression profiles of steroidogenic enzymes and steroidogenesis-related factors during the process of degeneration and sex reversal of ovary of ovarian *cyp19a1*

1278 mutants, revealed by RNAseq. The expression of major transcripts of *cyp19a1* (A),
1279 *cyp19a2* (B), *foxl2* (C), *ad4bp/sf-1* (D), *star* (E), *cyp11a1* (F), *hsd3b* (G), *hsd11b* (H),
1280 *srd5a1* (I), *cyp17* (J) and *hsd17bs* (K) are shown. Phase 1 is ovarian RNA sampled
1281 before initiation of degeneration of the ovary. Phase 2 is RNA from ovaries
1282 displaying degeneration of ovarian follicles (thick granulosa cell layer), but with fin
1283 morphology of the female type. Phase 3 is RNA obtained during degeneration of
1284 ovarian follicle when the external phenotype had changed to the male type. The Y
1285 axis indicates expression quantity as RPKM (Reads per kilobase of exon per million
1286 mapped reads). Asterisks in A, C and D-I, and "a", "b", "c" in J and K indicate
1287 significant differences when comparing two samples with the TCC package.
1288
1289 Figure 10
1290 Summary diagram of function of estrogens in maintenance of ovarian
1291 differentiation in medaka. (A) In wild type adult ovary, germline stem cells and
1292 their *Sox9a2*-positive supporting cells differentiate into ovarian follicle continuously.
1293 (B) In the *cyp19a1* mutant ovary, gonads differentiated into ovaries according to
1294 genetic sex. Ovarian follicles of mutants developed to the same size as secondary
1295 vitellogenic-sized follicle in non-mutants but did not accumulate yolk. Ovarian
1296 follicles then under degeneration. In mutant ovaries, genes associated with the
1297 synthesis of non-aromatizable androgens were highly up-regulated. At an age when
1298 wild type females were initiating vitellogenesis, supporting cells of the *cyp19a1*
1299 mutant differentiated into Sertoli cells. Sertoli cell-derived *gsdf* could induce the
1300 differentiation of germline stem cells into spermatogonia. Spermatogenesis
1301 proceeded normally and functional sperm were produced. Taking all the evidence
1302 together, the data show that estrogens are critical for the maintenance of

differentiation of germline stem cells into oogonia and accumulation of yolk in secondary vitellogenic follicles. Estrogen deficiency and/or imbalance in the ratio of estrogens and androgens may stimulate sex reversal of adult ovary.

A

ATCGGCATGAACGAGAAGGGAATCATATTTAACAACAATGTGGCTTTA
I G M N E K G I I F N N N V A L

TGGAAAAAGATTCGTACCTATTTCACCAAAGCTTTGACTGGGCCAAAC
W K K I R T Y F T K A L T G P N

TAA
K164X

CTGCAGCAAACAGTGGAAGTTTGCGTCACCTCCACACAGACTCACCTG
L Q Q T V E V C V T S T Q T H L

TAG
Q183X

GACAACCTGAGCAGTTTGTCTTACGTGGACGTC
D N L S S L S Y V D V

B

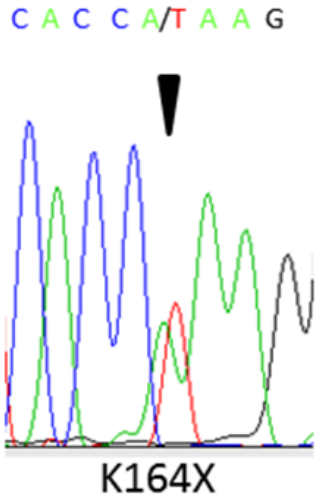

K164X

C

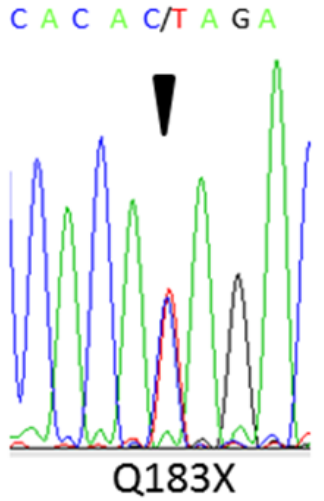

Q183X

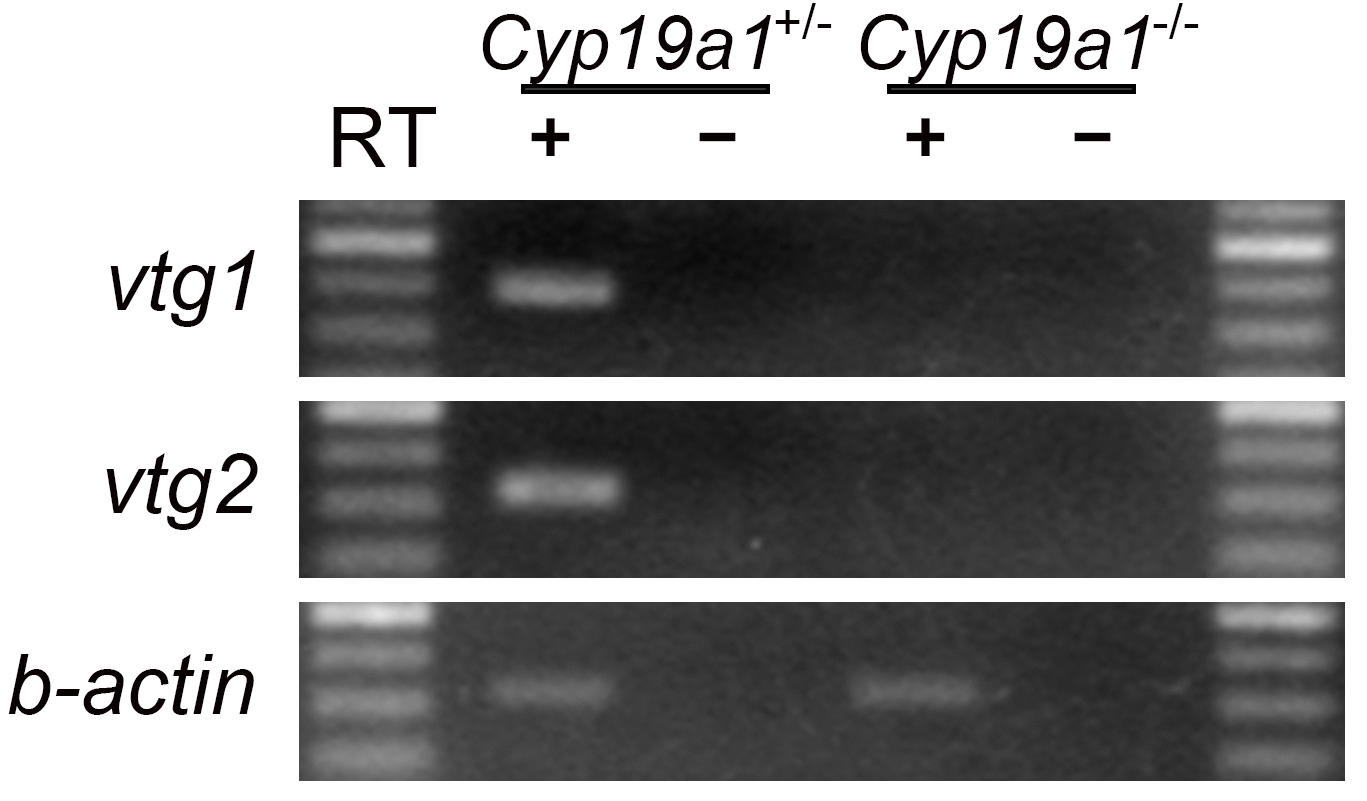
Cyp19a1+/-
Cyp19a1-/-
RT
+
–
+
–
vtg1
vtg2
b-actin

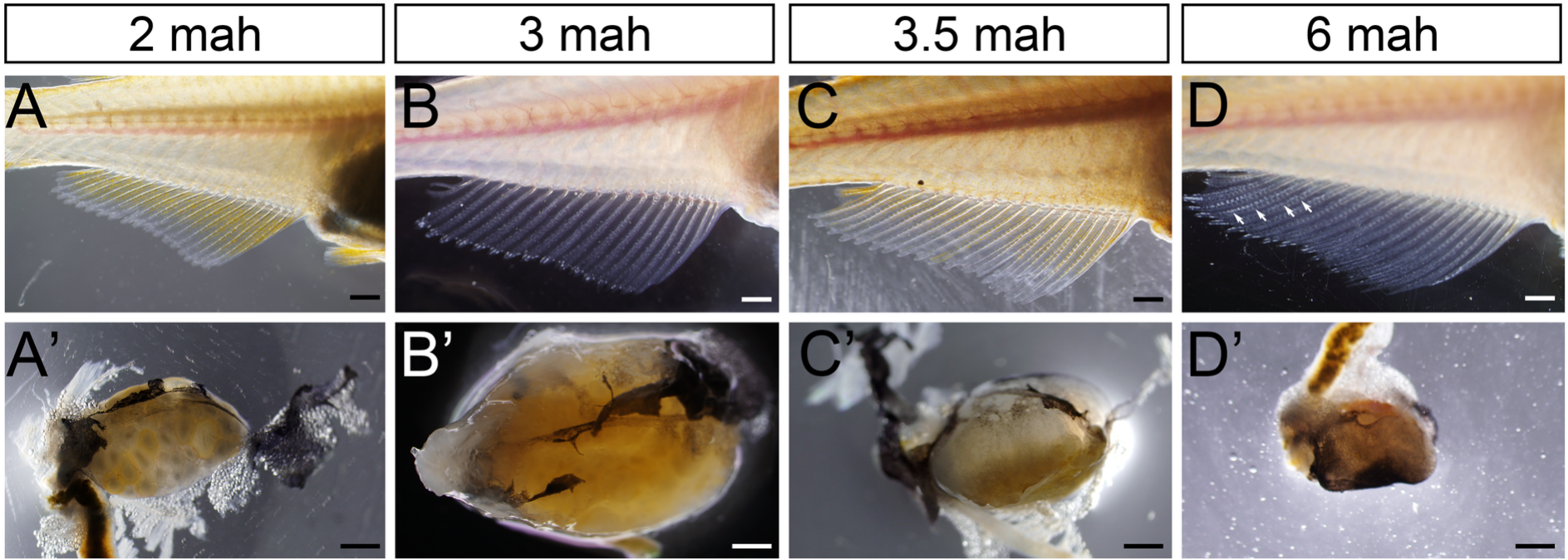
2 mah
3 mah
3.5 mah
6 mah
A
B
C
D
A'
B'
C'
D'

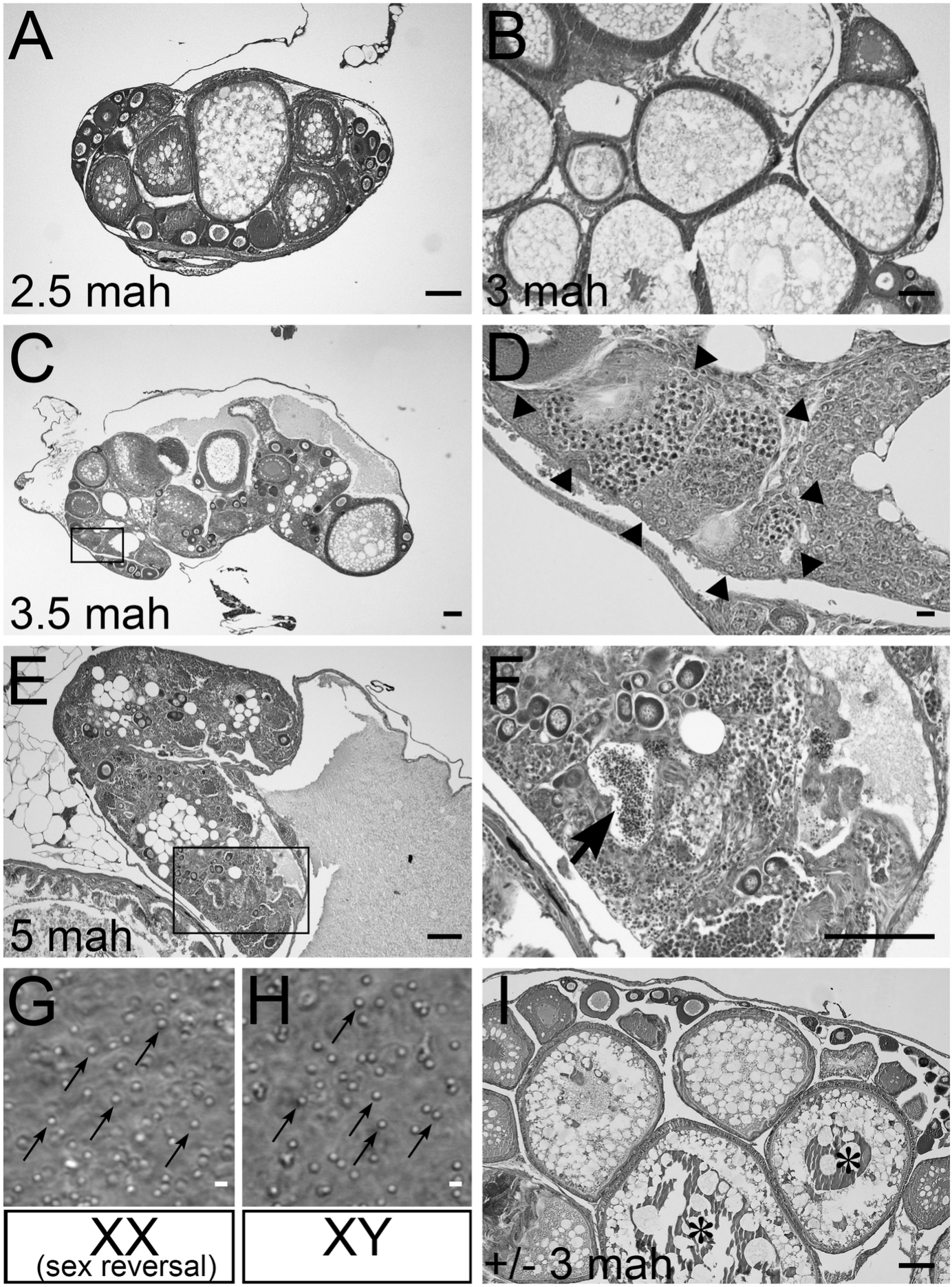
A
2.5 mah
B
3 mah
C
3.5 mah
D
E
5 mah
F
G
H
XX
(sex reversal)
XY
I
+/- 3 mah

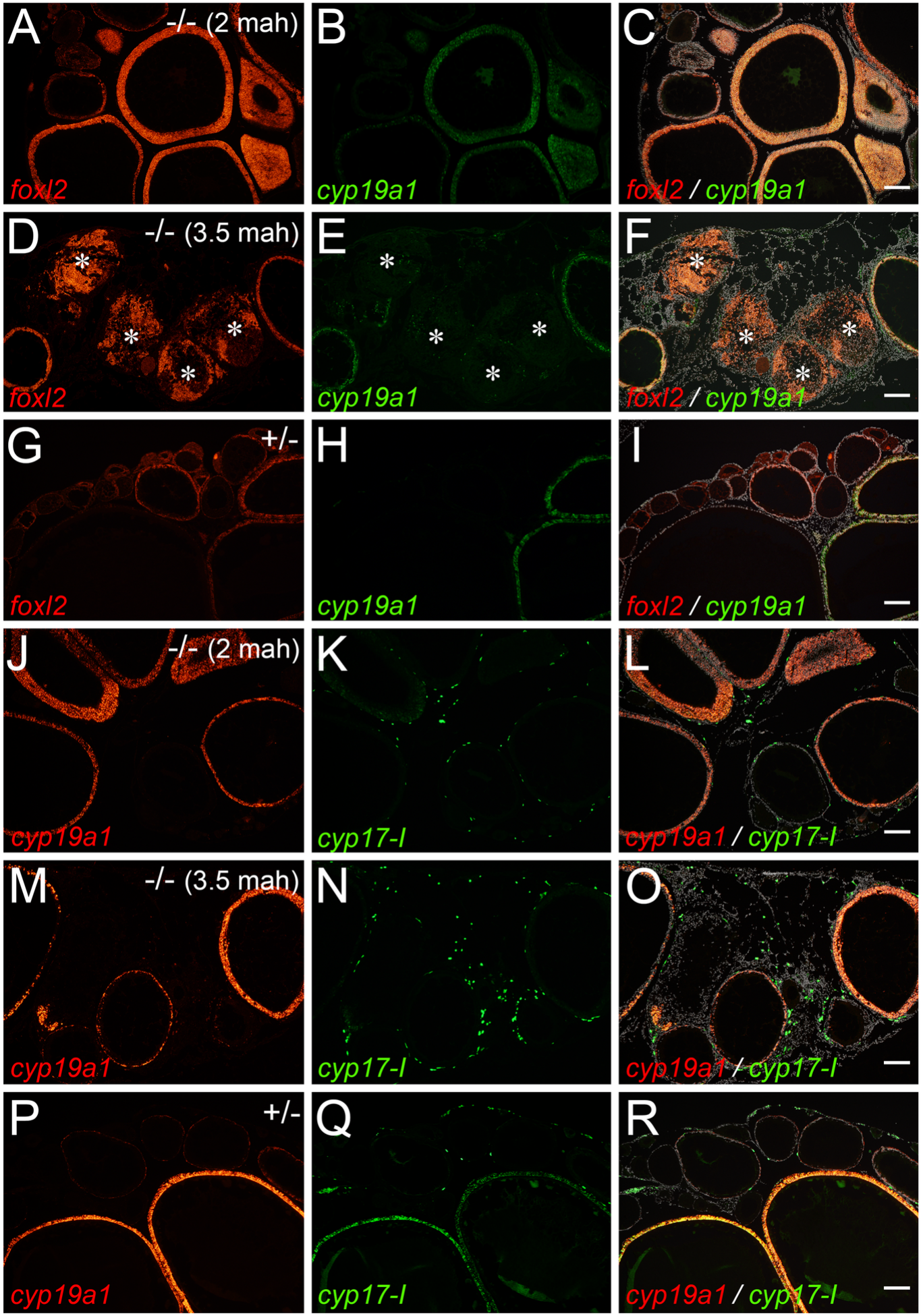
A
-/- (2 mah)
foxl2
B
cyp19a1
C
foxl2 / cyp19a1
D
-/- (3.5 mah)
foxl2
E
cyp19a1
F
foxl2 / cyp19a1
G
+/-
foxl2
H
cyp19a1
I
foxl2 / cyp19a1
J
-/- (2 mah)
cyp19a1
K
cyp17-I
L
cyp19a1 / cyp17-I
M
-/- (3.5 mah)
cyp19a1
N
cyp17-I
O
cyp19a1 / cyp17-I
P
+/-
cyp19a1
Q
cyp17-I
R
cyp19a1 / cyp17-I

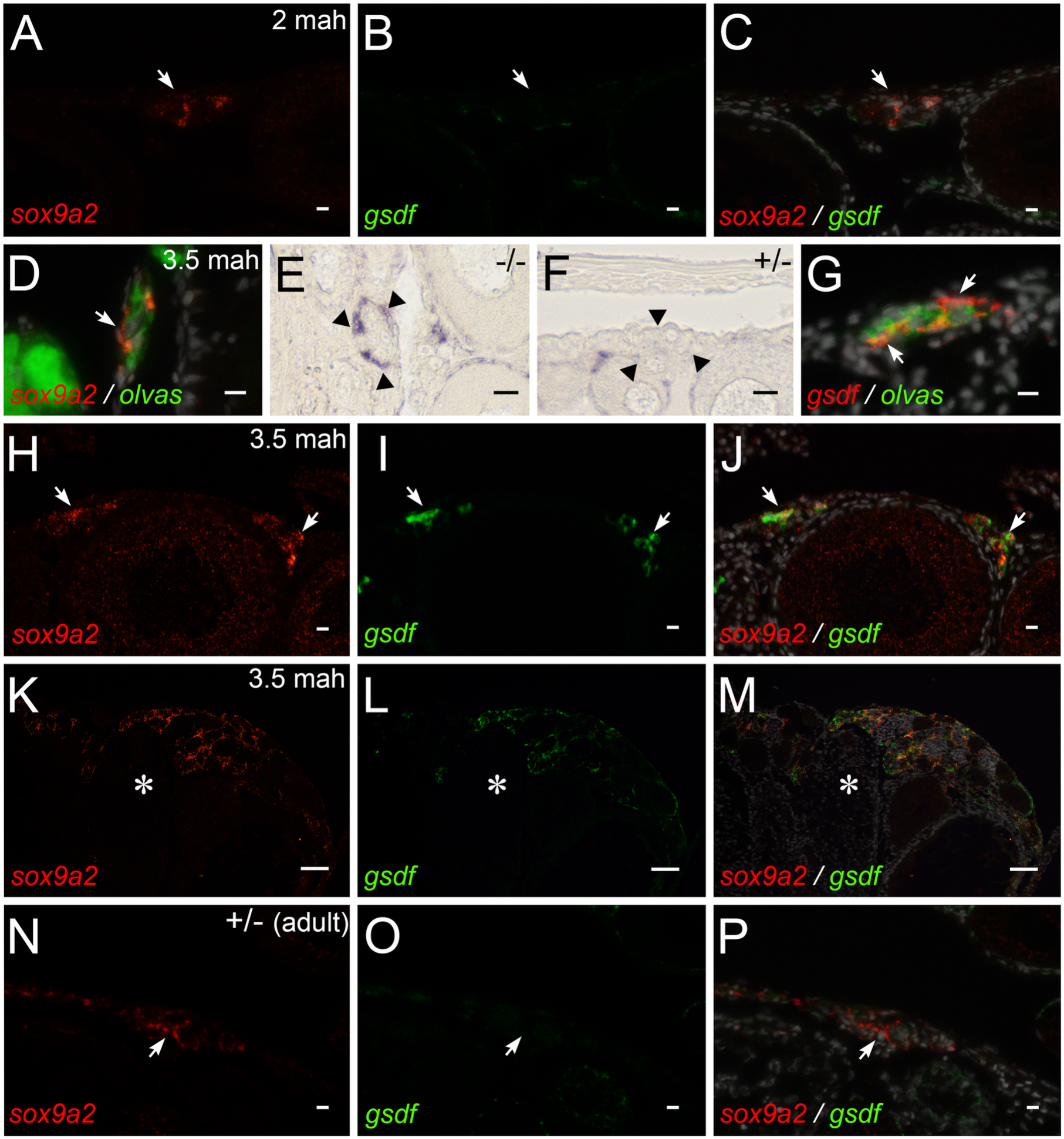
A
2 mah
sox9a2
B
gsdf
C
sox9a2 / gsdf
D
3.5 mah
sox9a2 / olvas
E
-/-
F
+/-
G
gsdf / olvas
H
3.5 mah
sox9a2
I
gsdf
J
sox9a2 / gsdf
K
3.5 mah
sox9a2
L
gsdf
M
sox9a2 / gsdf
N
+/- (adult)
sox9a2
O
gsdf
P
sox9a2 / gsdf

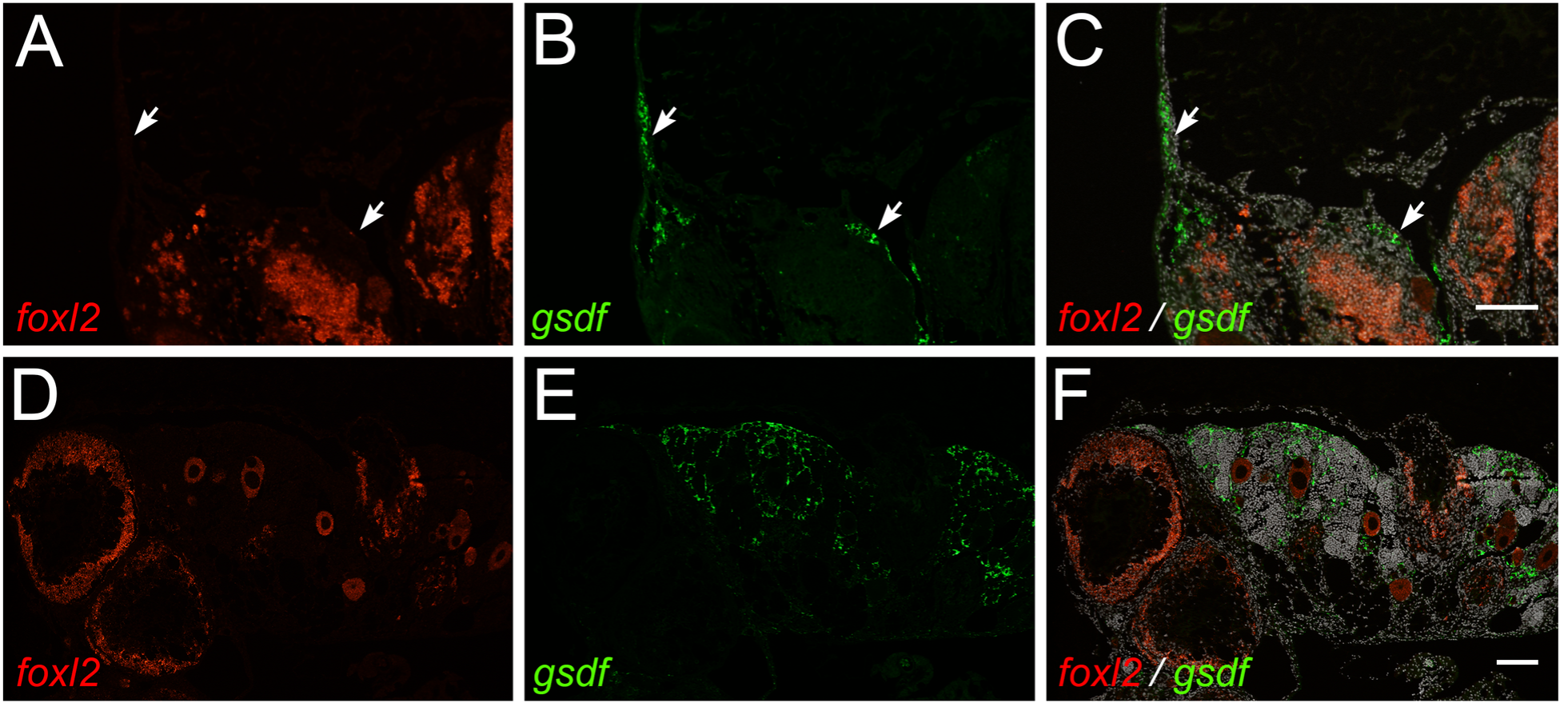
A
foxl2
B
gsdf
C
foxl2 / gsdf
D
foxl2
E
gsdf
F
foxl2 / gsdf

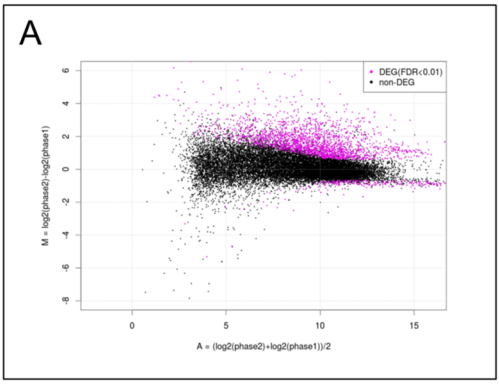
A
DEG(FDR<0.01)
non-DEG
M = log2(phase2)-log2(phase1)
A = (log2(phase2)+log2(phase1))/2

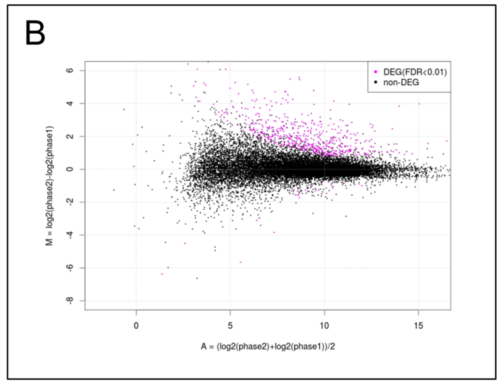
B
DEG(FDR<0.01)
non-DEG
M = log2(phase2)-log2(phase1)
A = (log2(phase2)+log2(phase1))/2

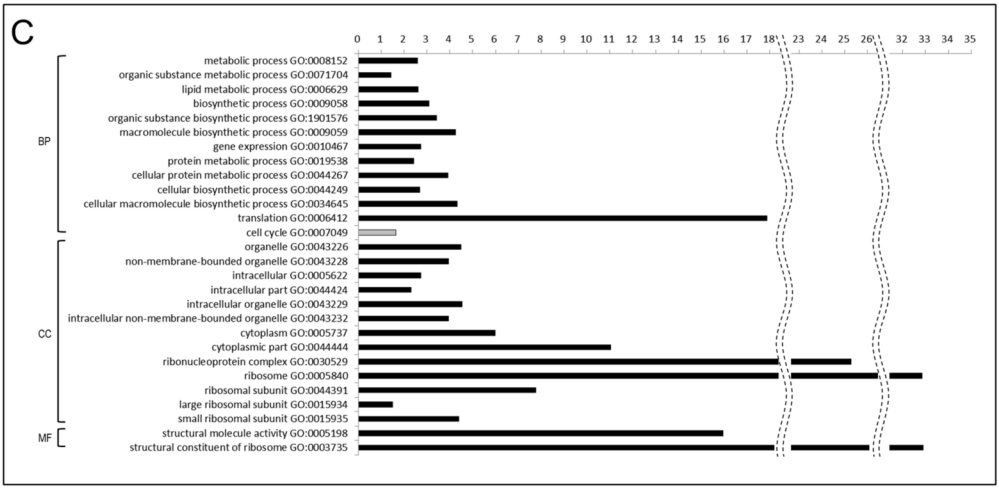
C
BP
CC
MF
metabolic process GO:0008152
organic substance metabolic process GO:0071704
lipid metabolic process GO:0006629
biosynthetic process GO:0009058
organic substance biosynthetic process GO:1901576
macromolecule biosynthetic process GO:0009059
gene expression GO:0010467
protein metabolic process GO:0019538
cellular protein metabolic process GO:0044267
cellular biosynthetic process GO:0044249
cellular macromolecule biosynthetic process GO:0034645
translation GO:0006412
cell cycle GO:0007049
organelle GO:0043226
non-membrane-bounded organelle GO:0043228
intracellular GO:0005622
intracellular part GO:0044424
intracellular organelle GO:0043229
intracellular non-membrane-bounded organelle GO:0043232
cytoplasm GO:0005737
cytoplasmic part GO:0044444
ribonucleoprotein complex GO:0030529
ribosome GO:0005840
ribosomal subunit GO:0044391
large ribosomal subunit GO:0015934
small ribosomal subunit GO:0015935
structural molecule activity GO:0005198
structural constituent of ribosome GO:0003735

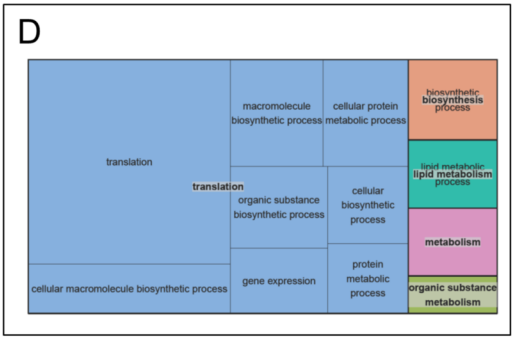
D
translation
macromolecule biosynthetic process
cellular protein metabolic process
biosynthetic process
translation
organic substance biosynthetic process
cellular biosynthetic process
lipid metabolic process
metabolism
cellular macromolecule biosynthetic process
gene expression
protein metabolic process
organic substance metabolism

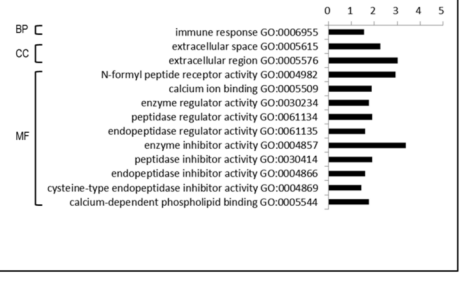
E
BP
CC
MF
immune response GO:0006955
extracellular space GO:0005615
extracellular region GO:0005576
N-formyl peptide receptor activity GO:0004982
calcium ion binding GO:0005509
enzyme regulator activity GO:0030234
peptidase regulator activity GO:0061134
endopeptidase regulator activity GO:0061135
enzyme inhibitor activity GO:0004857
peptidase inhibitor activity GO:0030414
endopeptidase inhibitor activity GO:0004866
cysteine-type endopeptidase inhibitor activity GO:0004869
calcium-dependent phospholipid binding GO:0005544

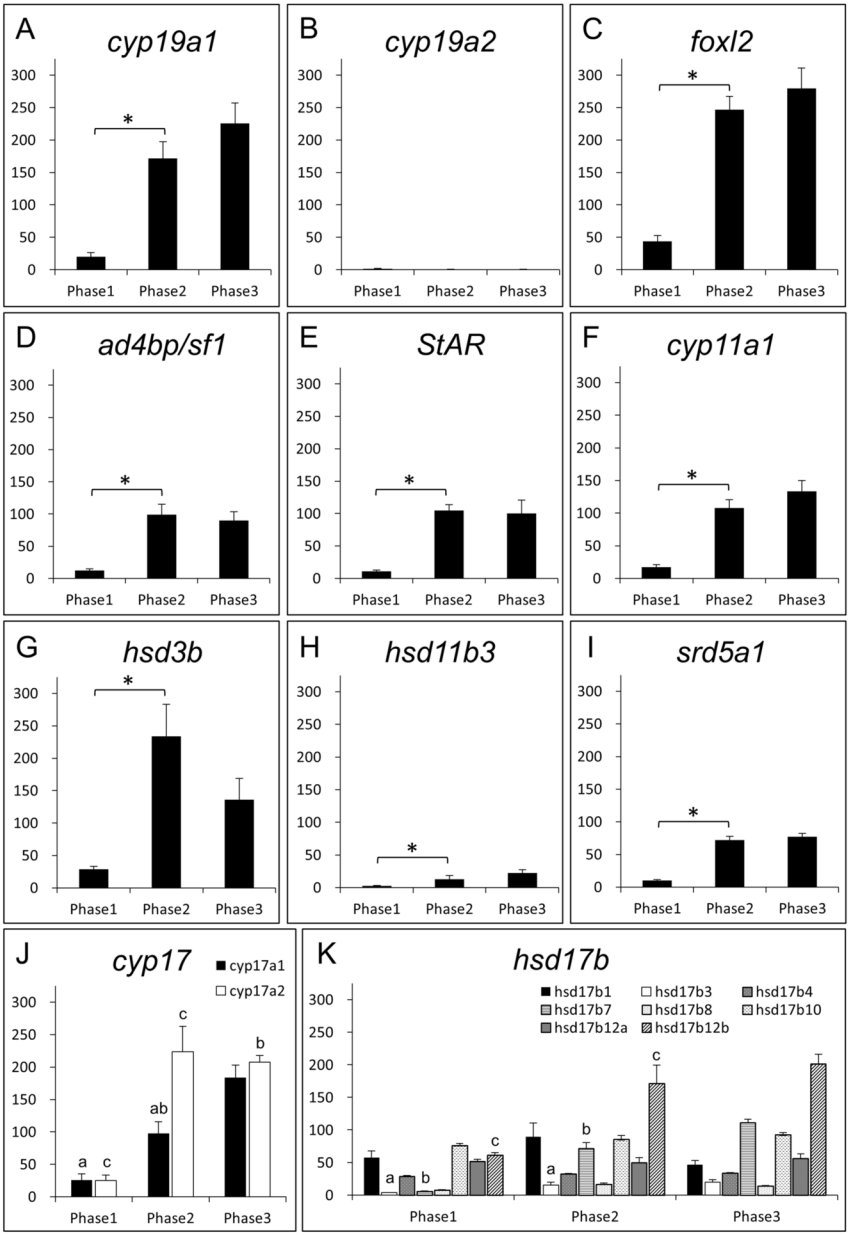
A
cyp19a1
B
cyp19a2
C
foxl2
D
ad4bp/sf1
E
StAR
F
cyp11a1
G
hsd3b
H
hsd11b3
I
srd5a1
J
cyp17
cyp17a1
cyp17a2
K
hsd17b
hsd17b1
hsd17b3
hsd17b4
hsd17b7
hsd17b8
hsd17b10
hsd17b12a
hsd17b12b
Phase1
Phase2
Phase3

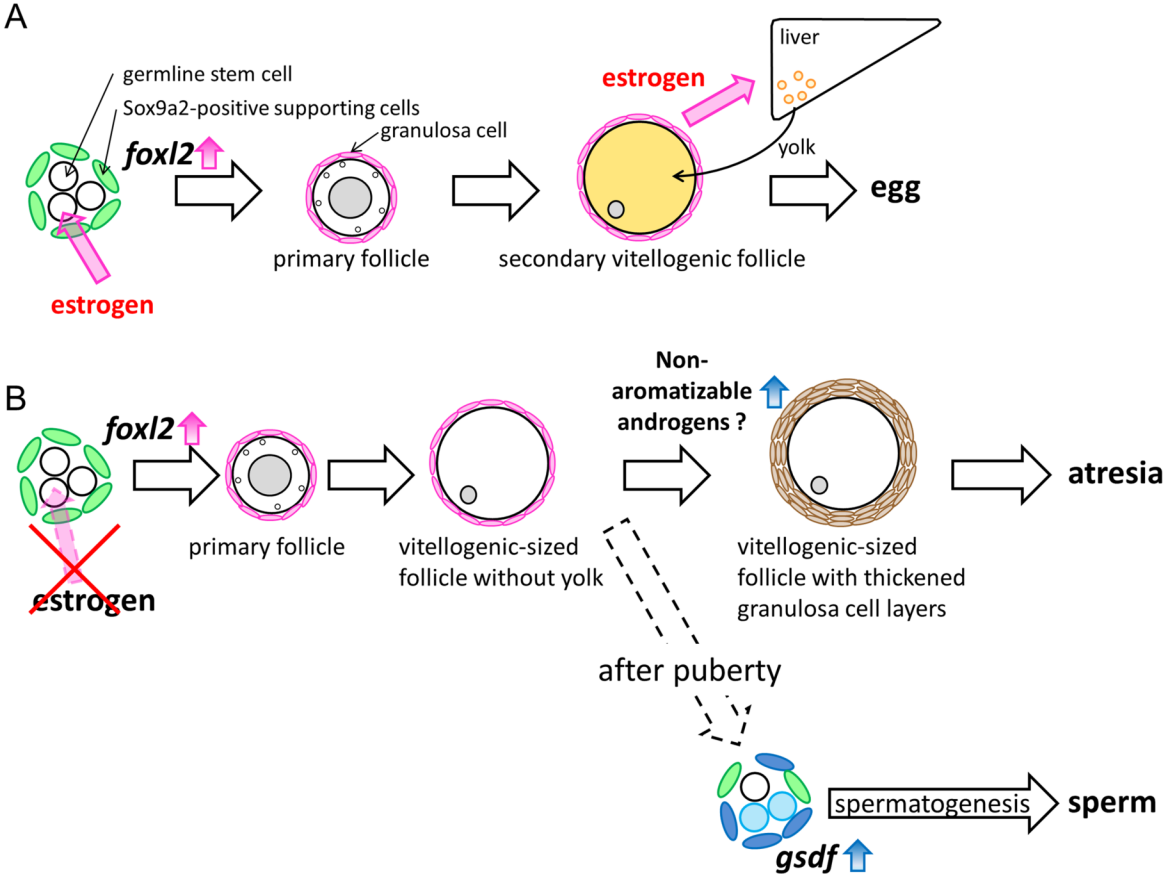
A
germline stem cell
Sox9a2-positive supporting cells
foxl2
granulosa cell
primary follicle
estrogen
liver
estrogen
yolk
egg
secondary vitellogenic follicle
estrogen
B
foxl2
primary follicle
vitellogenic-sized
follicle without yolk
Non-
aromatizable
androgens ?
vitellogenic-sized
follicle with thickened
granulosa cell layers
atresia
estrogen
after puberty
spermatogenesis
sperm
gsdf

Table 1 measurements of estrogen in aromatase mutant ovary by radioimmunoassay.

XX arom +/-

Sample No.	(pg/gonad)
1	69.9
2	95.3
3	85.1
4	71.5
mean	80.4 (±6.0 S.E.)

XX arom -/- ovary

Sample No.	(pg/gonad)
1	Below Detection Limit
2	Below Detection Limit
3	Below Detection Limit
4	16.9

The minimum detectable limit (ED80): 31 pg/ml.

Table 2 Top 15 up-regulated genes based on FDR from RNA-seq comparison of ovaries before degeneration and ovaries with degenerating follicle obtained from medaka displaying a female external phenotype.

Ensembl ID	gene name	log fold-chage	FDR
ENSORLT00000018892	HSD17B7 (hydroxysteroid (17-beta) dehydrogenase 7)	3.55	8.73×10^{-40}
ENSORLT00000023596	plod1a (procollagen-lysine 1, 2-oxoglutarate 5-dioxygenase 1a)	2.34	6.60×10^{-29}
ENSORLT00000017714	Uncharacterized protein	6.03	7.74×10^{-29}
ENSORLT00000004491	txndc12 (thioredoxin domain containing 12 (endoplasmic reticulum))	2.24	7.74×10^{-29}
ENSORLT00000017993	srd5a1 (steroid-5-alpha-reductase, alpha polypeptide 1 (3-oxo-5 alpha-steroid delta 4-dehydrogenase alpha 1))	2.75	1.76×10^{-26}
ENSORLT00000021264	LPL (Uncharacterized protein)	3.90	1.1 x10-24
ENSORLT00000009427	slc26a10 (solute carrier family 26, member 10)	4.57	1.18×10^{-24}
ENSORLT00000003608	dmxl2 (Dmx-like 2)	2.67	4.54×10^{-24}
ENSORLT00000009736	gba2 (glucosidase, beta (bile acid) 2)	2.56	5.07×10^{-23}
ENSORLT00000006000	MFF (mitochondrial fission factor)	4.43	1.50×10^{-21}
ENSORLT00000008593	scdb (stearoyl-CoA desaturase b)	3.47	3.95×10^{-21}
ENSORLT00000006606	camsap1a (calmodulin regulated spectrin-associated protein 1a)	16.44	4.60×10^{-20}
ENSORLT00000003242	si:ch211-274p24.3	3.96	5.44×10^{-20}
ENSORLT00000017705	Uncharacterized protein	4.10	8.20×10^{-20}
ENSORLT00000021651	rcn3 (reticulocalbin 3, EF-hand calcium binding domain)	2.68	1.63×10^{-19}

Table 3 Top 15 down-regulated genes based on FDR from RNA-seq comparison of ovaries before degeneration and ovaries with degenerating follicle obtained from medaka displaying a female external phenotype.

Ensembl ID	gene name	log fold-chage	FDR
ENSORLT00000006001	MFF (mitochondrial fission factor)	-4.67	2.10×10^{-8}
ENSORLT00000022374	nqo1 (NAD(P)H dehydrogenase, quinone 1)	-1.19	4.05×10^{-6}
ENSORLT00000011943	abi1b (abl-interactor 1b)	-14.20	5.39×10^{-6}
ENSORLT00000020246	sfrp1 (secreted frizzled-related protein 1)	-5.32	0.000045
ENSORLT00000018561	Uncharacterized protein	-0.99	0.000057
ENSORLT00000003654	cldnd (claudin d)	-1.16	0.000082
ENSORLT00000008109	ipo4 (importin 4)	-16.68	0.000105
ENSORLT00000013433	zgc:154054	-0.97	0.000187
ENSORLT00000011902	GABRA2 (gamma-aminobutyric acid (GABA) A receptor, alpha 2)	-1.06	0.000195
ENSORLT00000011592	LONRF3 (LON peptidase N-terminal domain and ring finger 3)	-14.93	0.000213
ENSORLT00000006696	Uncharacterized protein	-1.35	0.000231
ENSORLT00000009437	h2afx (H2A histone family, member X)	-1.03	0.000243
ENSORLT00000017016	n4bp1 (nedd4 binding protein 1)	-15.52	0.000245
ENSORLT00000006017	gba3 (glucosidase, beta, acid 3 (gene/pseudogene))	-1.08	0.000269
ENSORLT00000019298	olmt2-mmp (membrane-type matrix metalloproteinase)	-13.03	0.000282

Table 4 Top 15 up-regulated genes based on FDR from RNA-seq comparison of ovaries with degenerating follicle obtained from medaka displaying a female external phenotype, with ovaries with degenerating follicles obtained from medaka displaying a male external phenotype.

Ensembl ID	gene name	log fold-chage	FDR
ENSORLT00000001345	LGALS4 (lectin, galactoside-binding, soluble, 4)	5.49	1.54×10^{-24}
ENSORLT00000015483	C1S (complement component 1, s subcomponent)	2.91	4.81×10^{-23}
ENSORLT00000008629	cmklr1 (chemokine-like receptor 1)	3.40	4.81×10^{-23}
ENSORLT00000022415	mrc1b (mannose receptor, C type 1b)	2.94	8.93×10^{-23}
ENSORLT00000004575	slc43a3b (solute carrier family 43, member 3b)	2.57	1.50×10^{-21}
ENSORLT00000025881	spp1 (secreted phosphoprotein 1)	5.45	7.33×10^{-21}
ENSORLT00000009824	f13a1b (coagulation factor XIII, A1 polypeptide b)	2.24	1.41×10^{-20}
ENSORLT00000008068	CLEP (Uncharacterized protein)	3.05	1.76×10^{-20}
ENSORLT00000016480	lrrc17 (leucine rich repeat containing 17)	2.97	3.80×10^{-20}
ENSORLT00000007402	si:dkey-211g8.1	4.32	1.03×10^{-18}
ENSORLT00000019682	ctsk (cathepsin K)	3.95	1.46×10^{-17}
ENSORLT00000005242	Uncharacterized protein	3.92	4.59×10^{-17}
ENSORLT00000025503	fn1 (fibronectin-1 precursor)	2.68	2.30×10^{-16}
ENSORLT00000018137	csf3r (colony stimulating factor 3 receptor (granulocyte))	2.68	2.39×10^{-16}
ENSORLT00000025222	AGPAT6 (1-acylglycerol-3-phosphate O-acyltransferase 6)	2.61	2.39×10^{-16}

Table 5 Top 15 down-regulated genes based on FDR from RNA-seq comparison of ovaries with degenerating follicle obtained from medaka displaying a female external phenotype, with ovaries with degenerating follicles obtained from medaka displaying a male external phenotype.

Ensembl ID	gene name	log fold-chage	FDR
ENSORLT00000020187	desma (desmin a)	-5.65	6.83×10^{-8}
ENSORLT00000005299	ARFIP2 (ADP-ribosylation factor interacting protein 2)	-10.15	2.54×10^{-6}
ENSORLT00000001210	Uncharacterized protein	-1.32	0.000067
ENSORLT00000017943	rpa2 (replication protein A2)	-8.00	0.000221
ENSORLT00000022167	Uncharacterized protein	-1.72	0.000239
ENSORLT00000018666	rorcb (RAR-related orphan receptor C b)	-1.47	0.000377
ENSORLT00000007049	p2ry11 (purinergic receptor P2Y, G-protein coupled, 11)	-7.90	0.000421
ENSORLT00000005615	tyw3 (tRNA-yW synthesizing protein 3 homolog (S. cerevisiae))	-6.67	0.000534
ENSORLT00000012133	zgc:173961	-1.14	0.000589
ENSORLT00000025735	Uncharacterized protein	-0.99	0.000781
ENSORLT00000002523	si:dkey-23k10.5	-3.10	0.000791
ENSORLT00000000998	evpla (envoplakin a)	-1.27	0.000808
ENSORLT00000011161	gem (GTP binding protein overexpressed in skeletal muscle)	-2.54	0.000915
ENSORLT00000011471	SPOCK2 (sparc/osteonectin, cwcv and kazal-like domains proteoglycan (testican) 2)	-3.84	0.001045
ENSORLT00000025255	Uncharacterized protein	-1.56	0.001583